
Symmetry-Based Perspectives on Hamiltonian Quantum Search Algorithms and Schrödinger's Dynamics between Orthogonal States

Carlo Cafaro¹ and James Schneeloch²

¹*University at Albany-SUNY, Albany, NY 12222, USA and*

²*Air Force Research Laboratory, Information Directorate, Rome, New York, 13441, USA*

It is known that the continuous-time variant of Grover's search algorithm is characterized by quantum search frameworks that are governed by stationary Hamiltonians, which result in search trajectories confined to the two-dimensional subspace of the complete Hilbert space formed by the source and target states. Specifically, the search approach is ineffective when the source and target states are orthogonal.

In this paper, we employ normalization, orthogonality, and energy limitations to demonstrate that it is unfeasible to breach time-optimality between orthogonal states with constant Hamiltonians when the evolution is limited to the two-dimensional space spanned by the initial and final states. Deviations from time-optimality for unitary evolutions between orthogonal states can only occur with time-dependent Hamiltonian evolutions or, alternatively, with constant Hamiltonian evolutions in higher-dimensional subspaces of the entire Hilbert space. Ultimately, we employ our quantitative analysis to provide meaningful insights regarding the relationship between time-optimal evolutions and analog quantum search methods. We determine that the challenge of transitioning between orthogonal states with a constant Hamiltonian in a sub-optimal time is closely linked to the shortcomings of analog quantum search when the source and target states are orthogonal and not interconnected by the search Hamiltonian. In both scenarios, the fundamental cause of the failure lies in the existence of an inherent symmetry within the system.

I. INTRODUCTION

Searching a marked item within an unstructured database by means of a continuous-time evolution, characterized by a running time proportional to \sqrt{N} , where N represents the dimension of the search space, is a significant endeavor in the realm of analog quantum computing [1–3]. Additionally, a highly beneficial objective in continuous-time quantum computation involves the development of Hamiltonian evolutions that can transition the system from specified initial states to final states in the shortest time possible [4–6]. A key distinction between analog quantum search and optimal time evolutions lies in the fact that, in the former scenario, the time evolution transpires between a known source state and an unknown target state. Conversely, in the latter scenario, the time evolution occurs between known initial and final states. Nevertheless, a crucial element common to both analog quantum search and optimal-time evolutions is the ability to restrict focus to the two-dimensional subspace of the complete N -dimensional Hilbert space [1, 7], which is defined by the source (initial) and target (final) states, as the objective is to achieve optimal Hamiltonian evolutions.

The initial continuous-time adaptation of Grover's original discrete quantum search algorithm [8–12] was introduced by Farhi and Gutmann in Ref. [1]. Afterwards, Bae and Kwon examined a generalization of the Farhi-Gutmann analog quantum search algorithm in Ref. [13]. Both quantum search Hamiltonians discussed in Refs. [1, 13] are independent of time. The shift from time-independence to time-dependence within the context of analog quantum search algorithms was initially proposed under the assumption of global adiabatic evolution in Ref. [14], and subsequently, in a more favorable context of local adiabaticity in Ref. [15]. In the local adiabatic evolution framework, the time-dependent search Hamiltonian is defined as a linear interpolation between two time-independent Hamiltonians. In this scenario, the system is initialized in the ground state of one of the two Hamiltonians. This Hamiltonian is then adiabatically transformed into the other Hamiltonian, whose ground state is presumed to represent the unknown solution to the search problem. The time-dependence of the Hamiltonian is captured by the time-dependent interpolation function. Notably, the specific form of this function can be established by enforcing the local adiabaticity condition at every moment during the quantum mechanical evolution of the system. In general terms, the adiabatic approximation posits that a system prepared in an instantaneous eigenstate of the Hamiltonian will remain close to this prepared state if the Hamiltonian undergoes changes at a sufficiently slow rate [16, 17]. Consequently, any functional form of the interpolation schedule that meets the requisite degree of slowness for the adiabatic condition to be satisfied can be formally regarded. Interestingly, there is no inherent reason to preclude a nonlinear interpolation of the two static Hamiltonians [18]. Indeed, Perez and Romanelli examined nonadiabatic quantum search Hamiltonians that are defined through a nonlinear interpolation of the two time-independent Hamiltonians referenced in Ref. [19]. They introduced two search algorithms that display distinct characteristics, depending on the parametric and temporal forms of the two interpolation functions utilized to establish the time-dependent Hamiltonian. Notably, both algorithms demonstrated

the characteristic $\mathcal{O}(\sqrt{N})$ Grover-like scaling behavior when locating the target state within an N -dimensional search space. However, one of the algorithms necessitated a specific time for measurement to identify the target state, exhibiting periodic oscillatory behavior akin to the original Grover search algorithm [8, 20, 21]. Conversely, the other algorithm led the source state to evolve asymptotically into a quantum state that significantly overlapped with the target state, showcasing monotonic behavior and resembling the fixed-point Grover search algorithm [9, 12].

When examining the efficiency of quantum-mechanical unitary evolutions defined by Hermitian Hamiltonians, under which an initial unit state vector transitions to a final unit state vector [22, 23], two primary alternative methodologies arise in the literature [4, 5]. The first methodology, proposed by Mostafazadeh in Ref. [4], involves seeking an expression for the Hamiltonian by maximizing the energy uncertainty of the quantum system. This initial approach is supported by the relationship between the angular velocity of the minimal-time evolution of the quantum system and the energy uncertainty. Conversely, the second methodology, introduced by Bender and colleagues in Ref. [5], aims to derive an expression for the Hamiltonian by minimizing the time required for the evolution from the initial to the final state, while ensuring that the difference between the largest and smallest eigenvalues of the Hamiltonian remains constant. Considering that the maximum energy uncertainty correlates with the difference between the largest and smallest energy eigenvalues, constraining the difference between the largest and smallest eigenvalues of the Hamiltonian effectively constrains the energy uncertainty. Consequently, it is reasonable to anticipate that these two quantum descriptions of geodesic Hamiltonian motion are fundamentally equivalent. Upon closer examination, it becomes evident that these two methodologies emphasize slightly different characteristics. Notably, the unique aspects of these two distinct methods for describing geodesic quantum evolutions were skillfully utilized in Ref. [24] to aid in delineating the formal analogies between the geometry of quantum evolutions exhibiting unit quantum geometric efficiency and the geometry of classical polarization optics for light waves, where the degree of polarization matches the degree of coherence between the electric vibrations in any two mutually orthogonal directions of wave propagation [25, 26]. While these distinguishing characteristics of Mostafazadeh's and Bender's methodologies were briefly mentioned in Ref. [24], a comprehensive comparative analysis of the two approaches found in Ref. [4] and Ref. [5] is presented in Ref. [27].

Symmetry arguments hold significant strength in various research domain [28], including quantum walks [29, 30], quantum transport [31], and quantum algorithms [32]. In Ref. [29], for example, the authors present the concept of a chiral quantum walk. This refers to a quantum walk on a graph or lattice where complex-valued couplings are incorporated into the Hamiltonian to create directionality and disrupt time-reversal symmetry. These complex phases afford enhanced control over quantum transport, facilitating phenomena such as near-perfect state transfer, directed excitation routing, and capabilities that exceed the fundamental limits of traditional, non-chiral quantum walks. In Ref. [31], instead, the authors investigate the manner in which the interaction between dissipative processes and an inherent symmetry propels the quantum system of interest towards a degenerate steady state. This state retains a portion of the information from the initial state, attributed to the absence of mixing among the various symmetry sectors. Consequently, this paves the way for comprehensive control over transport properties, including both the average current and its statistical characteristics, by manipulating this information through initial-state preparation methods. In Ref. [32], lastly, the authors introduce a symmetry-enhanced CD (counterdiabatic)-inspired variational ansatz tailored for qudit systems. They leverage the principle that the symmetries inherent in graph-defined problems can enhance the efficacy of VQAs (variational quantum algorithms) while simultaneously alleviating the demands on both classical and quantum hardware. By employing these symmetries, the authors effectively minimize the algorithm's resource requirements, particularly concerning the number of parameters, which currently poses a significant limitation for VQAs. Their ansatz strategically utilizes the system's symmetries to markedly decrease the quantity of free parameters available for optimization.

In the realm of analog quantum searching utilizing time-independent Hamiltonians, the search strategy encounters failure when the source and target states are orthogonal [1]. Similarly, in the context of optimal-time evolutions, it is impossible to evolve in a two-dimensional space in a time suboptimal manner between two orthogonal states using a stationary Hamiltonian [7]. Driven by these two shortcomings in the presence of orthogonal states, this paper aims to enhance our comprehension of the unique characteristics of continuous-time evolutions between orthogonal quantum states. More specifically, a partial list of questions being explored includes:

- [i] Why do stationary continuous-time quantum search Hamiltonians fail to be effective when there is no quantum overlap between the source and target states?
- [ii] Do time-dependent search Hamiltonians mitigate work failures such as, for instance, failure of the algorithm to reach the target state? Alternatively, could the orthogonality between source and target states continue to present a challenge that leads to work failure during the search?
- [iii] What distinguishes quantum evolutions with stationary Hamiltonians between orthogonal initial and final states in the two-dimensional subspace defined by these states as particularly significant?

-
- [iv] Do deviations from stationarity facilitate the development of suboptimal Hamiltonian evolutions between orthogonal states?
 - [v] Is the failure to transition between orthogonal states with a constant Hamiltonian in a sub-optimal time related to the ineffectiveness of analog quantum search when the source and target states are orthogonal?

Properly addressing these questions is important because it can deepen our theoretical understanding of the common foundations underlying both the successes and failures of analog quantum searches and time-optimal quantum evolutions, grounded in first physical principles and symmetry arguments.

This rest of the paper is structured as follows. In Section II, we begin with a discussion of the essential features of relevant continuous-time quantum search Hamiltonians, followed by an outline of the main considerations from the perspective of energy constraints when formulating optimal-time Hamiltonians. In Section III, we employ normalization, orthogonality, and energy constraints to demonstrate that it is unfeasible to breach time-optimality between orthogonal states with constant Hamiltonians when the evolution is restricted to the two-dimensional space defined by the initial and final states. In Section IV, we present an analytical example that illustrates the potential for deviating from time-optimal evolution between orthogonal states within the two-dimensional subspace (of a larger Hilbert space) that they generate, taking into account that the Hamiltonian may change over time. In Section V, we offer physical insights into how one can avoid analog quantum search failures by drawing parallels with occurrences in standard quantum evolutions between specified initial and final states. Our concluding observations are found in Section VI. Lastly, technical details appear in Appendices A-C.

II. PRELIMINARIES

In this section, following the discussion of the key characteristics of pertinent continuous-time quantum search Hamiltonians, we outline the primary considerations from an energy-constraints viewpoint when developing optimal-time Hamiltonians.

A. Analog quantum search

Quantum search algorithms, such as Grover's quantum search scheme [8, 12], were first introduced within a digital quantum computation framework characterized by a discrete series of unitary logic gates. In contrast, Farhi and Gutmann employed an analog quantum computation approach to introduce an analog variant of Grover's original quantum search algorithm, wherein the quantum register's state experiences a continuous time evolution influenced by a suitably chosen driving Hamiltonian [1]. The fundamental concept of the continuous time search algorithm introduced by Farhi and Gutmann can be encapsulated as follows. Given a Hamiltonian that operates on an N -dimensional (where $N = 2^n$) complex vector space \mathcal{H}_2^n , which possesses a single non-zero eigenvalue $E \neq 0$ while all other eigenvalues are zero, the objective is to identify the eigenvector $|w\rangle$ corresponding to the eigenvalue E . The search concludes when the quantum system is confirmed to be in the state $|w\rangle$. By utilizing time-independent Hamiltonian evolutions, Farhi and Gutmann demonstrated that their algorithm necessitated a minimum search duration on the order of \sqrt{N} , thereby exhibiting the same complexity as Grover's original quantum search algorithm. The complete original Farhi-Gutmann quantum search Hamiltonian as detailed in [1] is given by

$$H_{\text{FG}} \stackrel{\text{def}}{=} H_w + H_d = E |w\rangle \langle w| + E |s\rangle \langle s|, \quad (1)$$

where $H_w \stackrel{\text{def}}{=} E |w\rangle \langle w|$ and $H_d \stackrel{\text{def}}{=} E |s\rangle \langle s|$ denote the oracle and driving Hamiltonians, respectively. The normalized states $|s\rangle$ and $|w\rangle$ represent the initial (source) and final (target) states, respectively. It is important to note that, in order to comprehend the analog search process, it is adequate to concentrate on the two-dimensional subspace formed by $|s\rangle$ and $|w\rangle$. The target state $|w\rangle$ is an arbitrarily selected (unknown) state from the unit sphere in \mathcal{H}_2^n , whereas the source state $|s\rangle$ is a suitably chosen normalized vector that is independent of $|w\rangle$. The source state $|s\rangle$ evolves in accordance with Schrödinger's evolution law, $|s\rangle \mapsto |\psi(t)\rangle \stackrel{\text{def}}{=} e^{-\frac{i}{\hbar} H_{\text{FG}} t} |s\rangle$. Furthermore, with no loss of generality, the quantum overlap $x \stackrel{\text{def}}{=} \langle w|s\rangle \neq 0$ can be assumed to be real and positive since any phase factor in the inner product between these two states can be ultimately inserted into the state $|s\rangle$. In addition, since it suffices to limit our attention to the two-dimensional subspace of \mathcal{H}_2^n spanned by $|s\rangle$ and $|w\rangle$, it is useful to introduce the orthonormal

basis $\{|w\rangle, |r\rangle\}$ with $|r\rangle \stackrel{\text{def}}{=} (1-x^2)^{-1/2}(|s\rangle - x|w\rangle)$ and $|s\rangle = x|w\rangle + \sqrt{1-x^2}|r\rangle$, respectively. Making use of the basis $\{|w\rangle, |r\rangle\}$, it happens that the probability $\mathcal{P}_{\text{FG}}(t)$ of finding the state $|w\rangle$ at time t reduces to [1],

$$\mathcal{P}_{\text{FG}}(t) \stackrel{\text{def}}{=} \left| \langle w | e^{-\frac{i}{\hbar} H_{\text{FG}} t} | s \rangle \right|^2 = \sin^2 \left(\frac{Ex}{\hbar} t \right) + x^2 \cos^2 \left(\frac{Ex}{\hbar} t \right). \quad (2)$$

Specifically, the earliest moment t_{FG} when the transition probability $\mathcal{P}_{\text{FG}}(t)$ in Eq. (2) assumes its maximum value $\mathcal{P}_{\text{FG}}^{\text{max}} = 1$ is given by,

$$t_{\text{FG}} \stackrel{\text{def}}{=} \frac{\hbar}{E} \frac{\pi}{2x}. \quad (3)$$

For later use, we emphasize that the energy dispersion of H_{FG} evaluated with respect to source state $|s\rangle$ is given by $\Delta E_{\text{FG}} \stackrel{\text{def}}{=} Ex\sqrt{1-x^2}$. When the target state $|w\rangle$ is considered to be a member of a collection of mutually orthonormal quantum states $\{|a\rangle\}$ $1 \leq a \leq N$ in \mathcal{H}_2^N , the source state $|s\rangle$ can be effectively selected as an equal superposition of the N quantum states $\{|a\rangle\}$. Consequently, $x = 1/\sqrt{N}$ and from Eq. (3) we observe that $t_{\text{FG}} \propto \sqrt{N}$. Therefore, similar to Grover's search, the Farhi-Gutmann algorithm necessitates a minimum search duration on the order of \sqrt{N} . Furthermore, by positing that the target state is an unknown member of a specified orthonormal basis $\{|a\rangle\}$ with $1 \leq a \leq N$ in \mathcal{H}_2^N that is generated with complete certainty, Farhi and Gutmann demonstrated that their algorithm is optimally short.

Despite the optimality of the Farhi-Gutmann quantum search Hamiltonian in Eq. (1) (in the sense that $t_{\text{FG}} \propto \sqrt{N} \simeq t_{\text{Grover}}$), Fenner pointed out in Ref. [33] that the unitary evolution operator $U_{\text{FG}}(t) = e^{-\frac{i}{\hbar} H_{\text{FG}} t}$ deviates significantly from the intermediate states attained in the original algorithm when Grover's iterate is applied. Furthermore, he demonstrated that it is possible to consider a different search Hamiltonian that can more accurately align with the actual iterations defining Grover's algorithm. Fenner's search Hamiltonian is defined as,

$$H_{\text{Fenner}} \stackrel{\text{def}}{=} \frac{2i}{E} [H_w, H_d] = 2iEx(|w\rangle\langle s| - |s\rangle\langle w|), \quad (4)$$

where H_w , H_d , and x are the same quantities introduced for H_{FG} in Eq. (4). After some algebra (for details, see Appendix A), it turns out that the analogue of the transition probability in Eq. (2) is given by

$$\mathcal{P}_{\text{Fenner}}(t) \stackrel{\text{def}}{=} \left| \langle w | e^{-\frac{i}{\hbar} H_{\text{Fenner}} t} | s \rangle \right|^2 = \left| x \cos \left(2x\sqrt{1-x^2} \frac{E}{\hbar} t \right) + \sqrt{1-x^2} \sin \left(2x\sqrt{1-x^2} \frac{E}{\hbar} t \right) \right|^2. \quad (5)$$

In particular, the shortest time t_{Fenner} when the transition probability $\mathcal{P}_{\text{Fenner}}(t)$ in Eq. (5) assumes its maximum value $\mathcal{P}_{\text{Fenner}}^{\text{max}} = 1$ is given by,

$$t_{\text{Fenner}} \stackrel{\text{def}}{=} \frac{\hbar}{E} \frac{\arccos(x)}{2x\sqrt{1-x^2}}. \quad (6)$$

Interestingly, we point out that the energy dispersion of H_{Fenner} evaluated with respect to source state $|s\rangle$ is given by $\Delta E_{\text{Fenner}} \stackrel{\text{def}}{=} 2Ex\sqrt{1-x^2}$. Therefore, keeping in mind that $\Delta E_{\text{Fenner}} = 2\Delta E_{\text{FG}}$, an energetically fair comparison of Eqs. (3) and (6) yields $t_{\text{FG}} \simeq t_{\text{Fenner}}$ in the limiting case in which $x \ll 1$.

After covering the fundamentals of (time-independent) analog quantum search Hamiltonians, we are now prepared to introduce the key aspects of optimal-time Hamiltonians.

B. Optimal-time evolutions

Following Refs. [4, 6], let us assume a traceless and stationary Hamiltonian H defined by a spectral decomposition of the form $H \stackrel{\text{def}}{=} E_1 |E_1\rangle\langle E_1| + E_2 |E_2\rangle\langle E_2|$, with $\langle E_1 | E_2 \rangle = \delta_{12}$ and $E_2 \geq E_1$. For clarity, we note that $\{|E_i\rangle\}_{i=1,2}$ and $\{E_i\}_{i=1,2}$ specify the eigenvectors and the eigenvalues of the constant Hamiltonian H . Furthermore, δ_{ij} denotes the Kronecker delta symbol, where $1 \leq i, j \leq 2$. In time-optimal scenarios, one is interested in the evolution of a state $|A\rangle$, not necessarily normalized, into a state $|B\rangle$ in the shortest possible time by maximizing the energy uncertainty ΔE ,

$$\Delta E \stackrel{\text{def}}{=} \left[\frac{\langle A | H^2 | A \rangle}{\langle A | A \rangle} - \left(\frac{\langle A | H | A \rangle}{\langle A | A \rangle} \right)^2 \right]^{1/2}, \quad (7)$$

so that ΔE in Eq. (7) equals ΔE_{\max} . The reason why one maximizes the energy uncertainty ΔE is justified by the fact that the speed of quantum evolution ds/dt along the curve that connects $|A\rangle$ to $|B\rangle$ is proportional to the energy uncertainty ΔE , $ds/dt \propto \Delta E$. What is the value of ΔE_{\max} ? To obtain this value, we notice that any unnormalized initial state $|A\rangle$ can be decomposed as $|A\rangle = \alpha_1 |E_1\rangle + \alpha_2 |E_2\rangle$ with generally complex quantum amplitudes $\alpha_1 \stackrel{\text{def}}{=} \langle E_1|A\rangle$ and $\alpha_2 \stackrel{\text{def}}{=} \langle E_2|A\rangle$. Using this decomposition of $|A\rangle$ into Eq. (7), we arrive at

$$\Delta E = \frac{E_2 - E_1}{2} \left[1 - \left(\frac{|\alpha_1|^2 - |\alpha_2|^2}{|\alpha_1|^2 + |\alpha_2|^2} \right)^2 \right]^{1/2}. \quad (8)$$

Inspection of Eq. (8) implies that the maximum value of ΔE in Eq. (8) is achieved when $|\alpha_1| = |\alpha_2|$. In particular, it equals

$$\Delta E_{\max} \stackrel{\text{def}}{=} \left(\frac{E_2 - E_1}{2} \right). \quad (9)$$

A fundamental concept in Mostafazadeh's methodology as presented in Ref. [4] involves the expression of $H \stackrel{\text{def}}{=} E_1 |E_1\rangle \langle E_1| + E_2 |E_2\rangle \langle E_2|$ in terms of the initial and final states $|A\rangle$ and $|B\rangle$, respectively, while ensuring that $\Delta E = \Delta E_{\max}$. In this context, it is important to recognize that $|A\rangle$ and $|B\rangle$ can be expressed as $|A\rangle = \alpha_1 |E_1\rangle + \alpha_2 |E_2\rangle$ and $|B\rangle = \beta_1 |E_1\rangle + \beta_2 |E_2\rangle$, respectively. Furthermore, it is necessary to impose $|\alpha_1| = |\alpha_2|$ and $|\beta_1| = |\beta_2|$ or, alternatively,

$$|\alpha_2|^2 - |\alpha_1|^2 = 0 = |\beta_2|^2 - |\beta_1|^2, \quad (10)$$

in order to meet the condition $\Delta E = \Delta E_{\max}$ and thereby ensure the minimum travel time $t_{AB}^{\min} \stackrel{\text{def}}{=} \hbar \arccos(|\langle A|B\rangle|) / \Delta E_{\max}$. After some straightforward but tedious algebra, one can show that the expression of the time-optimal Hamiltonian H that connects $|A\rangle$ to $|B\rangle$ (assuming energy dispersion $\Delta E = E$, with $E_2 = -E_1 \stackrel{\text{def}}{=} E$) is given by

$$H_{\text{opt}} \stackrel{\text{def}}{=} i\Delta E \frac{|\langle A|B\rangle|}{\sqrt{1 - |\langle A|B\rangle|^2}} \left[\frac{|B\rangle \langle A|}{\langle A|B\rangle} - \frac{|A\rangle \langle B|}{\langle B|A\rangle} \right]. \quad (11)$$

Recalling that quantum states that vary by solely a global phase are physically equivalent, we stress for completeness the unitary time propagator $U_{\text{opt}}(t) \stackrel{\text{def}}{=} e^{-\frac{i}{\hbar} H_{\text{opt}} t}$ is such that $U_{\text{opt}}(t_{\text{opt}}) |A\rangle = |B\rangle$ with $t_{\text{opt}} = t_{AB}^{\min}$ given by

$$t_{\text{opt}} \stackrel{\text{def}}{=} \frac{\hbar \arccos(|\langle A|B\rangle|)}{\Delta E}. \quad (12)$$

Finally, we remark that for H_{opt} in Eq. (11), one correctly obtains $\langle A|H_{\text{opt}}|A\rangle / \langle A|A\rangle = 0$ and $\Delta E = [\langle A|H_{\text{opt}}^2|A\rangle / \langle A|A\rangle]^{1/2} = E = \Delta E_{\max}$.

From a time-evolution standpoint, we stress that the word “*optimality*” means that the duration of the evolution from known initial and final states happens in an optimal time given by $t_{\text{opt}}^{\text{evolution}} = \hbar \arccos[|\langle A|B\rangle|] / \Delta E$. From a quantum search viewpoint, instead, “*optimality*” signifies that producing an unknown target state $|w\rangle$ starting from a known source state $|s\rangle$ happens in a temporal duration that is within a constant $c \in \mathbb{R}_+ \setminus \{0\}$ of the best possible. In other words, $t_{\text{opt}}^{\text{search}} \propto \sqrt{N}$, with N denoting the dimensionality of the search space. Interestingly, the time evolution sub-optimality of the Fahri-Gutmann search Hamiltonian can also be understood in geometric terms by re-deriving the search Hamiltonian from the point of view of quantum simulation (for details, see Appendix B). H_{FG} is time suboptimal and, therefore, cannot work for orthogonal states. H_{Fenner} , instead, is time optimal. However, it does not work for orthogonal states by construction.

Having addressed the basics of constructing optimal-time Hamiltonians, we are now prepared to explore deviations from time-optimality within two-dimensional subspaces.

III. OUR VERIFICATION

In this section, we utilize normalization, orthogonality, and energy constraints to illustrate that it is impractical to violate time-optimality between orthogonal states with constant Hamiltonians when the evolution is confined to the two-dimensional space spanned by the initial and final states.

Prior to outlining our energy-based arguments, we will briefly examine the geometric reasoning put forth by Brody in Ref. [7].

A. Geometry-based reasoning

What is the peculiarity of quantum evolutions between orthogonal quantum states in two-dimensional subspaces of the full Hilbert space when the unitary time propagator is specified by a time-independent Hamiltonian?

Following the analysis in Ref. [7], the peculiarity is that if one assumes two-dimensional motion with a constant Hamiltonian, the only way to evolve between orthogonal initial and final unit states $|A\rangle$ and $|B\rangle$ is along a time-optimal geodesic path. Why does this happen? First, since the states are orthogonal, they are antipodal on the two-sphere. Second, if $|A\rangle$ is a point on the projective line specified by a pair of eigenstates ($|E_+\rangle$, $|E_-\rangle$) of the Hamiltonian H , then the trajectory $\gamma(t)$ given by

$$\gamma(t) : t \mapsto |\psi(t)\rangle \stackrel{\text{def}}{=} U(t)|A\rangle = e^{-\frac{i}{\hbar}Ht}|A\rangle \quad (13)$$

never leaves the above mentioned projective line. Therefore, the length of the path between the antipodal states $|A\rangle$ and $|B\rangle \stackrel{\text{def}}{=} |\psi(t_{\text{final}})\rangle = U(t_{\text{final}})|A\rangle$ is π . Indeed, the (geodesic) length $\mathcal{L}[\gamma(t)]_{0 \leq t \leq t_{\text{final}}}$ of the path $\gamma(t)$ in Eq. (13) with $0 \leq t \leq t_{\text{final}}$ as measured by the Fubini-Study metric is given by (for details, see Appendix C)

$$\mathcal{L}[\gamma(t)]_{0 \leq t \leq t_{\text{final}}} = 2 \arccos [|\langle A|B\rangle|], \quad (14)$$

where $|A\rangle \stackrel{\text{def}}{=} |\psi(0)\rangle$ and $|B\rangle \stackrel{\text{def}}{=} |\psi(t_{\text{final}})\rangle$ [6]. Then, since the path length is π for any pair of energy eigenstates ($|E_+\rangle$, $|E_-\rangle$) that may specify other constant Hamiltonians, there exists no alternative path with a length longer than π . As a side note, we wish to clarify that the projective line connecting two points $|P_1\rangle$ and $|P_2\rangle$ is defined as the line whose points signify the entirety of normalized superpositions of the states $|P_1\rangle$ and $|P_2\rangle$. With a slight deviation from strict terminology, we interchangeably use the terms ‘‘points’’ and ‘‘states’’. Nevertheless, it is crucial to remember that these ‘‘points’’ are constituents of the projective Hilbert space $\mathcal{P}(\mathcal{H})$ (i.e., the space of rays) equipped with the Fubini-Study metric. The concept of a ‘‘ray’’ as an equivalence class of state vectors in the Hilbert space \mathcal{H} addresses the issue that global phase factors are physically insignificant, resulting in \mathcal{H} possessing an inherently redundant complex degree of freedom. For further information, we direct the reader to [7]. Therefore, when regarded as points on the projective line specified by ($|E_+\rangle$, $|E_-\rangle$), the unit state vectors $|A\rangle$ and $|B\rangle$ can be decomposed as

$$|A\rangle = \langle E_+|A\rangle|E_+\rangle + \langle E_-|A\rangle|E_-\rangle, \text{ and } |B\rangle = \langle E_+|B\rangle|E_+\rangle + \langle E_-|B\rangle|E_-\rangle, \quad (15)$$

respectively. In particular, normalization of $|A\rangle$ and $|B\rangle$ implies $|\langle E_+|A\rangle|^2 + |\langle E_-|A\rangle|^2 = 1$ and $|\langle E_+|B\rangle|^2 + |\langle E_-|B\rangle|^2 = 1$, respectively. In particular, when $|A\rangle$ and $|B\rangle$ are orthogonal and, in addition, $H = E_+|E_+\rangle\langle E_+| + E_-|E_-\rangle\langle E_-|$ is stationary, the only possible scenario is $|\langle E_+|A\rangle|^2 = |\langle E_-|A\rangle|^2 = 1/2$ and $|\langle E_+|B\rangle|^2 = |\langle E_-|B\rangle|^2 = 1/2$.

In conclusion, the distinctive feature of orthogonal states $|A\rangle$ and $|B\rangle$ is that their relative distance, defined by the Fubini-Study metric, consistently measures π (irrespective of the pair of energy eigenstates one may choose to examine). Conversely, for nonorthogonal states $|A\rangle$ and $|B\rangle$, it is generally observed that the relative distance between them on different projective lines (determined by appropriate pairs of energy eigenstates linked to specific stationary Hamiltonians) tends to vary. For straightforward illustrative examples displaying optimal and suboptimal Hamiltonian evolutions between nonorthogonal quantum states on the Bloch sphere, we recommend consulting Ref. [34].

Following a concise examination of the geometric rationale put forth by Brody to elucidate the absence of paths exceeding π in length between orthogonal states, when the evolution is limited to the two-dimensional subspace they span, we are now ready to present our alternative perspective based on energy considerations.

B. Energy-based reasoning

In the following, we present our alternative approach to clarify the lack of paths longer than π in length that connect orthogonal states, particularly when the evolution is confined to the two-dimensional subspace they occupy.

Let us assume an arbitrary parametrization of the unit state vectors $|A\rangle$ and $|B\rangle$ given by,

$$|A\rangle = \alpha_1|E_1\rangle + \alpha_2|E_2\rangle, \text{ and } |B\rangle = \beta_1|E_1\rangle + \beta_2|E_2\rangle, \quad (16)$$

respectively, where α_1 , α_2 , β_1 , and β_2 are complex quantum amplitudes. In particular, we assume in Eq. (16) that the spectral decomposition of the Hamiltonian restricted to the two-dimensional subspace spanned by $|A\rangle$ and $|B\rangle$ is given by $H = E_1|E_1\rangle\langle E_1| + E_2|E_2\rangle\langle E_2|$. The states $|A\rangle$ and $|B\rangle$ have to satisfy both normalization (i.e., $\langle A|A\rangle = 1 = \langle B|B\rangle$) and orthogonality conditions (i.e., $\langle A|B\rangle = 0 = \langle B|A\rangle$). Therefore, it must be

$$|\alpha_1|^2 + |\alpha_2|^2 = 1 = |\beta_1|^2 + |\beta_2|^2, \quad (17)$$

and

$$\alpha_1^* \beta_1 + \alpha_2^* \beta_2 = 0 = \alpha_1 \beta_1^* + \alpha_2 \beta_2^*, \quad (18)$$

respectively. Most importantly, since we want to connect $|A\rangle$ to $|B\rangle$ via a unitary time-propagator $U(t) = e^{-\frac{i}{\hbar}Ht}$, there must exist an instant t_{final} such that $|B\rangle = e^{-\frac{i}{\hbar}Ht_{\text{final}}} |A\rangle$. Therefore, given that $|B\rangle = e^{-\frac{i}{\hbar}Ht_{\text{final}}} |A\rangle$ with H time-independent, it must be

$$\langle A | H | A \rangle = \langle B | H | B \rangle, \quad (19)$$

and, in particular,

$$\Delta E_A^2 \stackrel{\text{def}}{=} \langle A | H^2 | A \rangle - \langle A | H | A \rangle^2 = \langle B | H^2 | B \rangle - \langle B | H | B \rangle^2 \stackrel{\text{def}}{=} \Delta E_B^2. \quad (20)$$

The condition on the mean energy in Eq. (19) implies

$$E \left(|\alpha_2|^2 - |\alpha_1|^2 \right) = E \left(|\beta_2|^2 - |\beta_1|^2 \right), \quad (21)$$

that is,

$$|\alpha_2|^2 - |\alpha_1|^2 = |\beta_2|^2 - |\beta_1|^2. \quad (22)$$

Moreover, the condition on the energy variance in Eq. (20) leads to

$$E^2 \left[1 - \left(|\alpha_2|^2 - |\alpha_1|^2 \right)^2 \right] = E^2 \left[1 - \left(|\beta_2|^2 - |\beta_1|^2 \right)^2 \right], \quad (23)$$

that is,

$$\left(|\alpha_2|^2 - |\alpha_1|^2 \right)^2 = \left(|\beta_2|^2 - |\beta_1|^2 \right)^2. \quad (24)$$

We observe that the condition in Eq. (22) implies the condition in Eq. (24) (but not vice versa). Therefore, in summary, we have that the complex amplitudes α_1 , α_2 , β_1 , and β_2 must simultaneously satisfy the following set of constraints

$$\begin{cases} |\alpha_1|^2 + |\alpha_2|^2 = 1 = |\beta_1|^2 + |\beta_2|^2 \\ |\alpha_2|^2 - |\alpha_1|^2 = |\beta_2|^2 - |\beta_1|^2 \\ \alpha_1^* \beta_1 + \alpha_2^* \beta_2 = 0 = \alpha_1 \beta_1^* + \alpha_2 \beta_2^* \end{cases}. \quad (25)$$

Without loss of generality, we can set

$$|\alpha_2|^2 - |\alpha_1|^2 = \varepsilon = |\beta_2|^2 - |\beta_1|^2, \quad (26)$$

with $\varepsilon \in \mathbb{R}$ at this stage. We stress that the conditions in Eq. (26) represent the key departure from what is supposed to happen in a time-optimal setting as summarized in Eq. (10). Then, using the fact that $|\alpha_1|^2 + |\alpha_2|^2 = 1 = |\beta_1|^2 + |\beta_2|^2$, we get from the first two conditions in Eq. (25) that

$$|\alpha_1|^2 = \frac{1-\varepsilon}{2}, \quad |\alpha_2|^2 = \frac{1+\varepsilon}{2}, \quad |\beta_1|^2 = \frac{1-\varepsilon}{2}, \quad \text{and} \quad |\beta_2|^2 = \frac{1+\varepsilon}{2}, \quad (27)$$

with $\varepsilon \in (0, 1)$ (given the positivity of both $|\alpha_1|^2$ and $|\beta_1|^2$). As a side remark, we observe that when $\varepsilon = 0$, we recover the time-optimal scenario parametrization of the states $|A\rangle$ and $|B\rangle$ in Eq. (16). Returning to our discussion, making use of Eqs. (16) and (27), we can recast $|A\rangle$ and $|B\rangle$ in Eq. (16) as

$$|A\rangle = \sqrt{\frac{1-\varepsilon}{2}} e^{i\varphi_{\alpha_1}} |E_1\rangle + \sqrt{\frac{1+\varepsilon}{2}} e^{i\varphi_{\alpha_2}} |E_2\rangle, \quad (28)$$

and,

$$|B\rangle = \sqrt{\frac{1-\varepsilon}{2}} e^{i\varphi_{\beta_1}} |E_1\rangle + \sqrt{\frac{1+\varepsilon}{2}} e^{i\varphi_{\beta_2}} |E_2\rangle, \quad (29)$$

respectively. Therefore, employing Eqs. (28) and (29), the orthogonality condition $\langle A|B\rangle = 0$ reduces to

$$\frac{1-\varepsilon}{2}e^{-i(\varphi_{\alpha_1}-\varphi_{\beta_1})} + \frac{1+\varepsilon}{2}e^{-i(\varphi_{\alpha_2}-\varphi_{\beta_2})} = 0. \quad (30)$$

With no loss of generality, let us put

$$e^{-i(\varphi_{\alpha_1}-\varphi_{\beta_1})} = a + ib, \text{ and } e^{-i(\varphi_{\alpha_2}-\varphi_{\beta_2})} = c + id, \quad (31)$$

with $a^2 + b^2 = 1 = c^2 + d^2$, where $a, b, c,$ and d belong to \mathbb{R} . Then, using Eq. (31), the complex constraint in Eq. (30) leads to the following two real constraints

$$\begin{cases} a(1-\varepsilon) + c(1+\varepsilon) = 0 \\ [b(1-\varepsilon) + d(1+\varepsilon)] = 0 \end{cases}. \quad (32)$$

From Eq. (32), we get (being $\varepsilon \in (0, 1)$)

$$a = -c\frac{1+\varepsilon}{1-\varepsilon}, \text{ and } b = -d\frac{1+\varepsilon}{1-\varepsilon}. \quad (33)$$

Then, since we must have $a^2 + b^2 = 1 = c^2 + d^2$ because of the normalization conditions, Eq. (33) yields

$$a^2 + b^2 = c^2 \left(\frac{1+\varepsilon}{1-\varepsilon}\right)^2 + d^2 \left(\frac{1+\varepsilon}{1-\varepsilon}\right)^2 = (c^2 + d^2) \left(\frac{1+\varepsilon}{1-\varepsilon}\right)^2 = c^2 + d^2. \quad (34)$$

Therefore, Eq. (34) is valid if and only if

$$\left(\frac{1+\varepsilon}{1-\varepsilon}\right)^2 = 1. \quad (35)$$

Finally, we have that the condition in Eq. (35) is satisfied only if $\varepsilon = 0$ (which specifies the time-optimal scenario). Note that for $\varepsilon = 0$, the orthogonality condition in Eq. (30) is satisfied by $\varphi_{\alpha_1} - \varphi_{\beta_1} = 0$ and $\varphi_{\alpha_2} - \varphi_{\beta_2} = \pi$. In particular, denoting $\varphi_{\alpha_2} = \varphi_{\alpha}$ and $\varphi_{\beta_2} = \varphi_{\beta}$, the states $|A\rangle$ and $|B\rangle$ in Eqs. (28) and (29) assume the form

$$|A\rangle = \frac{|E_1\rangle + e^{i\varphi_{\alpha}}|E_2\rangle}{\sqrt{2}}, \text{ and } |B\rangle = \frac{|E_1\rangle + e^{i\varphi_{\beta}}|E_2\rangle}{\sqrt{2}}, \quad (36)$$

with $\langle A|B\rangle = e^{-i\frac{\varphi_{\alpha}-\varphi_{\beta}}{2}} \cos[(\varphi_{\alpha} - \varphi_{\beta})/2]$ and, in addition,

$$|\langle E_1|A\rangle|^2 = \frac{1}{2} = |\langle E_2|A\rangle|^2, \text{ and } |\langle E_1|B\rangle|^2 = \frac{1}{2} = |\langle E_2|B\rangle|^2. \quad (37)$$

Therefore, we recover the scenario that specifies the time-optimal evolution. This concludes our energy-oriented explanation regarding the absence of paths exceeding π in length that link orthogonal states when their evolution is restricted to the two-dimensional subspace they inhabit.

In summary, the sole method to facilitate suboptimal evolutions between orthogonal states is to exit the two-dimensional motion or, alternatively, to consider time-varying Hamiltonians to remain within two dimensions. In the first scenario, one can create nongeodesic paths of length exceeding π with constant Hamiltonians. Conversely, in the second scenario, nongeodesic paths of length greater than π can be examined because the unitary evolution is defined by an initial state that intersects multiple projective lines prior to reaching $|B\rangle$, with these ‘‘instantaneous’’ lines determined by a time-dependent pair of energy eigenstates for the time-varying Hamiltonian under consideration. We refer to Fig. 1 for a sketch of the geometry of Bloch vectors for both time optimal and time suboptimal evolutions between orthogonal states specified by a constant and a nonstationary Hamiltonian, respectively.

The forthcoming section will focus on a detailed examination of the deviation from time-optimality when utilizing a nonstationary Hamiltonian, all while staying within a two-dimensional subspace.

IV. ESCAPING TIME-OPTIMALITY

In this section, we provide an analytical demonstration of a distinct example illustrating the possibility of deviating from the time-optimal evolution between orthogonal states within a two-dimensional subspace of a larger Hilbert space that they create, considering that the Hamiltonian may vary over time.

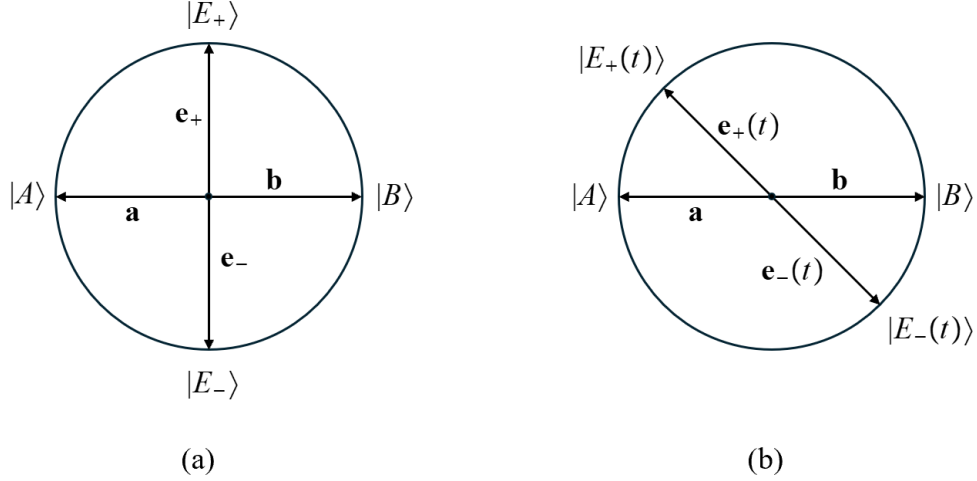


FIG. 1: In (a), there is sketch of the geometry of Bloch vectors for a time optimal evolution (with $\Delta E = \Delta E_{\max}$) between orthogonal states $|A\rangle$ and $|B\rangle$ specified by a constant Hamiltonian. In this case, we have $\mathbf{a} \cdot \mathbf{e}_- = 0 = \mathbf{a} \cdot \mathbf{e}_+$ and $\mathbf{b} \cdot \mathbf{e}_- = 0 = \mathbf{b} \cdot \mathbf{e}_+$. Clearly, $\mathbf{a} \cdot \mathbf{b} = -1 = \mathbf{e}_- \cdot \mathbf{e}_+$. In (b), there is sketch of the geometry of Bloch vectors for a time suboptimal evolution (with $\Delta E(t) < \Delta E_{\max}$) between orthogonal states $|A\rangle$ and $|B\rangle$ specified by a nonstationary Hamiltonian. In this case, we generally have $\mathbf{a} \cdot \mathbf{e}_-(t) \neq 0 = \mathbf{a} \cdot \mathbf{e}_+(t)$ and $\mathbf{b} \cdot \mathbf{e}_-(t) = 0 = \mathbf{b} \cdot \mathbf{e}_+(t)$. Clearly, $\mathbf{a} \cdot \mathbf{b} = -1 = \mathbf{e}_-(t) \cdot \mathbf{e}_+(t)$.

A. Preliminaries

In the subsequent discussion, we concentrate on single-qubit systems. In accordance with Ref. [35], our objective is to identify an appropriate time-dependent qubit Hamiltonian that propels the quantum system with optimal speed efficiency along a non-geodesic trajectory on the Bloch sphere (i.e., suboptimal geodesic efficiency). We note that the geodesic efficiency of a quantum evolution from $|A\rangle$ and $|B\rangle$ is defined as the ratio of the length of the geodesic path that connects $|A\rangle$ and $|B\rangle$ on the Bloch sphere to the length of the actual dynamical path produced by the system's Hamiltonian [22, 36, 37]. Conversely, the speed efficiency of a quantum evolution from $|A\rangle \stackrel{\text{def}}{=} |\psi(0)\rangle$ and $|B\rangle \stackrel{\text{def}}{=} |\psi(t_{\text{final}})\rangle$ is typically an instantaneous time-dependent quantity, where $0 \leq t \leq t_{\text{final}}$, and is characterized by the ratio of the energy uncertainty of the system (i.e., the energy expended during the quantum evolution) to the spectral norm of the Hamiltonian (i.e., the total energy of the system) [35].

In Ref. [35], the most comprehensive Hermitian nonstationary qubit Hamiltonian $H(t)$ is formulated in a way that it produces the identical motion $\pi(|\psi(t)\rangle)$ within the complex projective Hilbert space $\mathbb{C}P^1$ (or, correspondingly, on the Bloch sphere $S^2 \cong \mathbb{C}P^1$) as $|\psi(t)\rangle$, where the projection operator π is defined such that $\pi : \mathcal{H}_2^1 \ni |\psi(t)\rangle \mapsto \pi(|\psi(t)\rangle) \in \mathbb{C}P^1$. Generally, it can be demonstrated that $H(t)$ can be expressed as

$$H(t) = i\hbar |\partial_t m(t)\rangle \langle m(t)| - i\hbar |m(t)\rangle \langle \partial_t m(t)|, \quad (38)$$

where, for the sake of simplicity in notation, we can define $|m(t)\rangle = |m\rangle$, $|\partial_t m(t)\rangle = |\dot{m}\rangle$, and $\hbar = 1$. The unit state vector $|m\rangle$ satisfies the relations $\pi(|m(t)\rangle) = \pi(|\psi(t)\rangle)$ and $i\partial_t |m(t)\rangle = H(t)|m(t)\rangle$. The condition $\pi(|m(t)\rangle) = \pi(|\psi(t)\rangle)$ leads to the conclusion that $|m(t)\rangle = c(t)|\psi(t)\rangle$, with $c(t)$ denoting a complex function. By stipulating that $\langle m|m\rangle = 1$, we conclude that $|c(t)| = 1$. This subsequent condition indicates, in turn, that $c(t) = e^{i\phi(t)}$ for a certain real phase $\phi(t)$. Subsequently, by applying the parallel transport condition $\langle m|\dot{m}\rangle = \langle \dot{m}|m\rangle = 0$, the phase $\phi(t)$ is determined to be equal to $i \int \langle \psi|\dot{\psi}\rangle dt$. Consequently, $|m(t)\rangle = \exp(-\int_0^t \langle \psi(t')|\partial_{t'}\psi(t')\rangle dt') |\psi(t)\rangle$. It is important to note that $H(t)$ in Eq. (38) is inherently traceless, as it contains only off-diagonal elements within the orthogonal basis $\{|m\rangle, |\dot{m}\rangle\}$. Moreover, the condition $i\partial_t |m(t)\rangle = H(t)|m(t)\rangle$ indicates that $|m(t)\rangle$ adheres to the Schrödinger evolution equation. After providing some fundamental preliminary information regarding Uzdin's research in Ref. [35], we are now able to present our suggested time-dependent Hamiltonian.

B. Hamiltonian model

We start by examining a unit quantum state represented as

$$|\psi(t)\rangle = \cos(\omega_0 t) |0\rangle + e^{i\nu_0 t} \sin(\omega_0 t) |1\rangle, \quad (39)$$

where ν_0 and ω_0 are the two crucial real positive parameters that can be adjusted while investigating the quantum evolution. Recall that, using the polar and azimuthal angles $\theta(t)$ and $\varphi(t)$, respectively, an arbitrary state on the Bloch sphere can be expressed as $|\psi(t)\rangle = |\psi(\theta(t), \varphi(t))\rangle = \cos[\theta(t)/2] |0\rangle + e^{i\varphi(t)} \sin[\theta(t)/2] |1\rangle$. Consequently, we have $\omega_0 t = \theta(t)/2$ and $\nu_0 t = \varphi(t)$, which means $\omega_0 = \dot{\theta}/2$ and $\nu_0 = \dot{\varphi}$. Given that $\langle \psi(t) | \dot{\psi}(t) \rangle = i\nu_0 \sin^2(\omega_0 t) \neq 0$, it follows that $|\psi(t)\rangle$ is not parallel transported. Starting from the state $|\psi(t)\rangle$, we define the state $|m(t)\rangle \stackrel{\text{def}}{=} e^{-i\phi(t)} |\psi(t)\rangle$ with the phase $\phi(t)$ such that $\langle m(t) | \dot{m}(t) \rangle = 0$. A straightforward calculation shows that $\langle m(t) | \dot{m}(t) \rangle = 0$ if and only if $-i\dot{\phi} + \langle \psi(t) | \dot{\psi}(t) \rangle = 0$, which implies $\dot{\phi} = -i \langle \psi(t) | \dot{\psi}(t) \rangle$. By setting $\phi(0) = 0$, the temporal evolution of the phase $\phi(t)$ is described by

$$\phi(t) = \frac{\nu_0}{4\omega_0} [2\omega_0 t - \sin(2\omega_0 t)]. \quad (40)$$

Moreover, by utilizing Eq. (40), the parallel transported unit state $|m(t)\rangle$ is transformed into

$$|m(t)\rangle = e^{-i\phi(t)} |\psi(t)\rangle = e^{-i\frac{\nu_0}{4\omega_0} [2\omega_0 t - \sin(2\omega_0 t)]} [\cos(\omega_0 t) |0\rangle + e^{i\nu_0 t} \sin(\omega_0 t) |1\rangle]. \quad (41)$$

Note that $|A\rangle = |m(0)\rangle = |0\rangle$, whereas for $t_* = \pi/(2\omega_0)$ we find $|B\rangle = |m(t_*)\rangle \simeq |1\rangle$ (with “ \simeq ” denoting physical equivalence of quantum states, modulo unimportant global phase factors), leading to $\langle A|B\rangle = \langle B|A\rangle = 0$. Consequently, we equate the matrix representation of the Hamiltonian $\mathbb{H}(t) = i(|\dot{m}\rangle \langle m| - |m\rangle \langle \dot{m}|)$ in the orthogonal basis $\{|m\rangle, |\dot{m}\rangle\}$ to $\mathbb{H}(t) = h_0(t) \mathbf{I} + \mathbf{h}(t) \cdot \boldsymbol{\sigma}$, where $|m\rangle$ is defined in Eq. (41). Furthermore, by expressing $\rho(t) = |m(t)\rangle \langle m(t)| = (1/2) [\mathbf{I} + \mathbf{a}(t) \cdot \boldsymbol{\sigma}]$, we derive that the Bloch vector $\mathbf{a}(t)$ and the field vector $\mathbf{h}(t)$ become

$$\mathbf{a}(t) = \begin{pmatrix} \sin(2\omega_0 t) \cos(\nu_0 t) \\ \sin(\nu_0 t) \sin(2\omega_0 t) \\ \cos(2\omega_0 t) \end{pmatrix}, \quad (42)$$

and,

$$\mathbf{h}(t) = \begin{pmatrix} -\frac{\nu_0}{2} \cos(2\omega_0 t) \sin(2\omega_0 t) \cos(\nu_0 t) - \omega_0 \sin(\nu_0 t) \\ -\frac{\nu_0}{2} \cos(2\omega_0 t) \sin(2\omega_0 t) \sin(\nu_0 t) + \omega_0 \cos(\nu_0 t) \\ \frac{\nu_0}{2} \sin^2(2\omega_0 t) \end{pmatrix}, \quad (43)$$

respectively, with $h_0(t) = 0$. It is noteworthy to mention that the two real-valued three-dimensional vectors $\mathbf{a}(t)$ and $\mathbf{h}(t)$ presented in Eqs. (42) and (43), respectively, satisfy the vector differential equation $\dot{\mathbf{a}}(t) = 2\mathbf{h}(t) \times \mathbf{a}(t)$ [38, 39]. Indeed, up to constant factors, this vector differential equation describes the Larmor precession. This phenomenon is specified by the relation $d\mathbf{m}/dt = \gamma \mathbf{m} \times \mathbf{B}$, where \mathbf{m} is the magnetic moment vector, \mathbf{B} denotes the external magnetic moment, and γ is the gyromagnetic ratio.

Although the Hamiltonian models considered here are constructed from the quantum state $|\psi(t)\rangle = \cos[\alpha(t)] |0\rangle + e^{i\beta(t)} \sin[\alpha(t)] |1\rangle$ with $\alpha(t) \stackrel{\text{def}}{=} \omega_0 t$ and $\beta(t) \stackrel{\text{def}}{=} \nu_0 t$, our construction does not rely on this specific parametrization. It can be readily shown that the approach remains valid for more general parametrizations, where the parameters $\alpha(t)$ and $\beta(t)$ are not required to vary linearly in time. The particular choice adopted here was made solely for clarity of presentation.

C. Evolution of probabilities

Consider the Hamiltonian given by $\mathbb{H}(t) = i(|\dot{m}\rangle \langle m| - i|m\rangle \langle \dot{m}|)$, where $\langle m|m\rangle = 1$, $\langle m|\dot{m}\rangle = \langle \dot{m}|m\rangle = 0$, and $\langle \dot{m}|\dot{m}\rangle \neq 1$. With respect to the orthonormal basis $\mathcal{B} \stackrel{\text{def}}{=} \{|m\rangle, |\dot{m}\rangle / \sqrt{\langle \dot{m}|\dot{m}\rangle}\}$, we have

$$[\mathbb{H}]_{\mathcal{B}} = \begin{pmatrix} \langle m|\mathbb{H}|m\rangle & \frac{\langle m|\mathbb{H}|\dot{m}\rangle}{\sqrt{\langle \dot{m}|\dot{m}\rangle}} \\ \frac{\langle \dot{m}|\mathbb{H}|m\rangle}{\sqrt{\langle \dot{m}|\dot{m}\rangle}} & \frac{\langle \dot{m}|\mathbb{H}|\dot{m}\rangle}{\langle \dot{m}|\dot{m}\rangle} \end{pmatrix} = \begin{pmatrix} 0 & -i\sqrt{\langle \dot{m}|\dot{m}\rangle} \\ i\sqrt{\langle \dot{m}|\dot{m}\rangle} & 0 \end{pmatrix}. \quad (44)$$

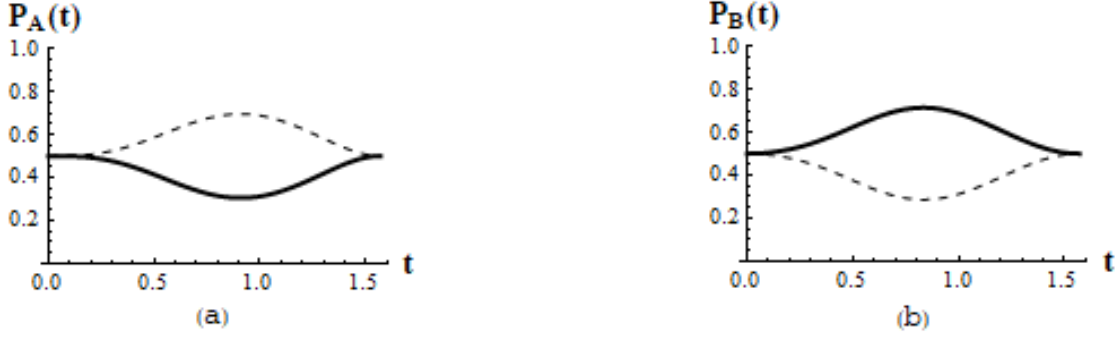


FIG. 2: In (a), there are the plots of the probabilities $P_A(t) \stackrel{\text{def}}{=} |\langle E_+(t) | A \rangle|^2$ (dashed line) and $P_A(t) \stackrel{\text{def}}{=} |\langle E_-(t) | A \rangle|^2$ (thick solid line) versus time t . In (b), there are the plots of the probabilities $P_B(t) \stackrel{\text{def}}{=} |\langle E_+(t) | B \rangle|^2$ (dashed line) and $P_B(t) \stackrel{\text{def}}{=} |\langle E_-(t) | B \rangle|^2$ (thick solid line) versus time t . In all plots, we set $\nu_0 = \omega_0 = 1$ and $0 \leq t \leq \pi/2$.

Searching for eigenvalues and eigenvectors of $[H]_B$ in Eq. (44), we find that they are given by

$$E_+(t) \stackrel{\text{def}}{=} +\sqrt{\langle \dot{m} | \dot{m} \rangle}, E_-(t) \stackrel{\text{def}}{=} -\sqrt{\langle \dot{m} | \dot{m} \rangle}, \quad (45)$$

and

$$|E_+(t)\rangle \stackrel{\text{def}}{=} \frac{1}{\sqrt{2}} \left[|m\rangle + i \frac{|\dot{m}\rangle}{\sqrt{\langle \dot{m} | \dot{m} \rangle}} \right], |E_-(t)\rangle \stackrel{\text{def}}{=} \frac{1}{\sqrt{2}} \left[|m\rangle - i \frac{|\dot{m}\rangle}{\sqrt{\langle \dot{m} | \dot{m} \rangle}} \right], \quad (46)$$

respectively. Note that, for the sake of convenience in notations, we have substituted $\{|E_1\rangle, |E_2\rangle\}$ with $\{|E_+\rangle, |E_-\rangle\}$. Therefore, the spectral decomposition of $H = i|\dot{m}\rangle\langle m| - i|m\rangle\langle \dot{m}|$ is given by

$$H(t) = E_+(t) |E_+(t)\rangle \langle E_+(t)| + E_-(t) |E_-(t)\rangle \langle E_-(t)|. \quad (47)$$

It is a straightforward to verify that $H(t) = i|\dot{m}\rangle\langle m| - i|m\rangle\langle \dot{m}|$ coincides with $H(t)$ in Eq. (47). Now, considering an evolution from $|A\rangle$ to $|B\rangle$ with $\langle A|B\rangle = \langle B|A\rangle = 0$ (and, additionally, assuming both states normalized to one), we have

$$|A\rangle = \langle E_+(t) | A \rangle |E_+(t)\rangle + \langle E_-(t) | A \rangle |E_-(t)\rangle, \text{ and } |B\rangle = \langle E_+(t) | B \rangle |E_+(t)\rangle + \langle E_-(t) | B \rangle |E_-(t)\rangle. \quad (48)$$

Using Eqs. (46) and (48), we notice that we generally obtain

$$|\langle E_+(t) | A \rangle|^2 = \frac{1}{2} \left| \langle m | A \rangle - i \frac{\langle \dot{m} | A \rangle}{\sqrt{\langle \dot{m} | \dot{m} \rangle}} \right|^2 \neq \frac{1}{2} \left| \langle m | A \rangle + i \frac{\langle \dot{m} | A \rangle}{\sqrt{\langle \dot{m} | \dot{m} \rangle}} \right|^2 = |\langle E_-(t) | A \rangle|^2, \quad (49)$$

with $|\langle E_+(t) | A \rangle|^2 + |\langle E_-(t) | A \rangle|^2 = 1$. More explicitly, taking $|A\rangle = |0\rangle$ and $|m\rangle = e^{-i\phi} [\cos(\alpha) |0\rangle + e^{i\beta} \sin(\alpha) |1\rangle]$ where $\alpha(t) \stackrel{\text{def}}{=} \omega_0 t$ and $\beta(t) \stackrel{\text{def}}{=} \nu_0 t$, the probability amplitude squared $|\langle E_+(t) | A \rangle|^2$ in Eq. (49) reduces to

$$|\langle E_+(t) | A \rangle|^2 = \frac{1}{2} \left| \left(\cos(\alpha) + \frac{\dot{\phi} \cos(\alpha)}{\sqrt{\dot{\alpha}^2 + \frac{1}{4} \dot{\beta}^2 \sin^2(2\alpha)}} \right) + i \frac{\dot{\alpha} \sin(\alpha)}{\sqrt{\dot{\alpha}^2 + \frac{1}{4} \dot{\beta}^2 \sin^2(2\alpha)}} \right|^2, \quad (50)$$

while $|\langle E_-(t) | A \rangle|^2$ in Eq. (49) becomes,

$$|\langle E_-(t) | A \rangle|^2 = \frac{1}{2} \left| \left(\cos(\alpha) - \frac{\dot{\phi} \cos(\alpha)}{\sqrt{\dot{\alpha}^2 + \frac{1}{4} \dot{\beta}^2 \sin^2(2\alpha)}} \right) - i \frac{\dot{\alpha} \sin(\alpha)}{\sqrt{\dot{\alpha}^2 + \frac{1}{4} \dot{\beta}^2 \sin^2(2\alpha)}} \right|^2. \quad (51)$$

Type of constraint	Optimal stationary evolution	Suboptimal nonstationary evolution
Path length	$s = \pi$	$s > \pi$
Energy uncertainty	$\Delta E = \Delta E_{\max}$	$\Delta E(t) < \Delta E_{\max}$
Probability amplitudes	$ \langle E_+ A \rangle ^2 = \frac{1}{2} = \langle E_- A \rangle ^2$	$ \langle E_+(t) A \rangle ^2 \neq \frac{1}{2} \neq \langle E_-(t) A \rangle ^2$
Bloch vectors	$\mathbf{a} \cdot \mathbf{e}_+ = 0 = \mathbf{a} \cdot \mathbf{e}_-$	$\mathbf{a} \cdot \mathbf{e}_+(t) \neq 0 \neq \mathbf{a} \cdot \mathbf{e}_-(t)$

TABLE I: Aspects of optimal stationary and suboptimal nonstationary Hamiltonian evolutions in terms of path lengths, energy uncertainties, probability amplitudes, and Bloch vector configurations.

As a side remark, one can easily verify by means of Eqs. (50) and (51) that $|\langle E_+(t) | A \rangle|^2 + |\langle E_-(t) | A \rangle|^2 = 1$ using some trigonometry and the fact that $\dot{\phi} = \dot{\beta} \sin^2(\alpha)$. Similarly, taking $|B\rangle = |1\rangle$ and $|m\rangle = e^{-i\phi} [\cos(\alpha) |0\rangle + e^{i\beta} \sin(\alpha) |1\rangle]$, use of Eqs. (46) and (48) yields probability amplitude squared $|\langle E_+(t) | B \rangle|^2$ and $|\langle E_-(t) | B \rangle|^2$ given by

$$|\langle E_+(t) | B \rangle|^2 = \frac{1}{2} \left| \left(\sin(\alpha) + \frac{\dot{\phi} \sin(\alpha) - \dot{\beta} \sin(\alpha)}{\sqrt{\dot{\alpha}^2 + \frac{1}{4} \dot{\beta}^2 \sin^2(2\alpha)}} \right) - i \frac{\dot{\alpha} \cos(\alpha)}{\sqrt{\dot{\alpha}^2 + \frac{1}{4} \dot{\beta}^2 \sin^2(2\alpha)}} \right|^2, \quad (52)$$

and,

$$|\langle E_-(t) | B \rangle|^2 = \frac{1}{2} \left| \left(\sin(\alpha) - \frac{\dot{\phi} \sin(\alpha) - \dot{\beta} \sin(\alpha)}{\sqrt{\dot{\alpha}^2 + \frac{1}{4} \dot{\beta}^2 \sin^2(2\alpha)}} \right) + i \frac{\dot{\alpha} \cos(\alpha)}{\sqrt{\dot{\alpha}^2 + \frac{1}{4} \dot{\beta}^2 \sin^2(2\alpha)}} \right|^2, \quad (53)$$

respectively. Again, one can check that $|\langle E_+(t) | B \rangle|^2 + |\langle E_-(t) | B \rangle|^2 = 1$ using some trigonometry and the fact that $\dot{\phi} = \dot{\beta} \sin^2(\alpha)$. For a plot of the transition probabilities in Eqs. (50), (51), (52), and (53), we refer to Fig. 2. Moreover, if we set $\rho_A \stackrel{\text{def}}{=} |A\rangle \langle A| = (\mathbf{1} + \mathbf{a} \cdot \boldsymbol{\sigma})/2$, $\rho_B \stackrel{\text{def}}{=} |B\rangle \langle B| = (\mathbf{1} + \mathbf{b} \cdot \boldsymbol{\sigma})/2$, $\rho_{E_{\pm}} \stackrel{\text{def}}{=} |E_{\pm}\rangle \langle E_{\pm}| = (\mathbf{1} + \mathbf{e}_{\pm} \cdot \boldsymbol{\sigma})/2$, and $\rho(t) \stackrel{\text{def}}{=} |\psi(t)\rangle \langle \psi(t)| = (\mathbf{1} + \mathbf{a}(t) \cdot \boldsymbol{\sigma})/2$, we note that $|\langle A | B \rangle|^2 = (\mathbf{1} + \mathbf{a} \cdot \mathbf{b})/2$ since $|\langle A | B \rangle|^2 = \text{tr}(\rho_A \rho_B) + 2\sqrt{\det(\rho_A) \det(\rho_B)}$. Therefore, in the stationary optimal-time evolution between orthogonal states $|A\rangle$ and $|B\rangle$, we have $\Delta E = \Delta E_{\max}$, $|\langle E_+ | A \rangle|^2 = 1/2 = |\langle E_- | A \rangle|^2$, $\mathbf{a} \cdot \mathbf{e}_+ = 0 = \mathbf{a} \cdot \mathbf{e}_-$, and the path length of the actual dynamical trajectory equals the length of the geodesic path (i.e., $s = s_{\text{geo}} = \theta_{AB} \stackrel{\text{def}}{=} 2 \arccos[|\langle A | B \rangle|] = \pi$, where $s \stackrel{\text{def}}{=} (2/\hbar) \int_{t_A}^{t_B} \Delta E(t') dt'$ [22]). Similar conditions in terms of probability amplitudes and Bloch vectors hold true for the final state $|B\rangle$ as well. Moreover, given that the Hamiltonian H remains constant, similar conditions are also fulfilled by $|\psi(t)\rangle$. From a geometric standpoint, the key aspect to highlight is the orthogonality between the Bloch vectors $\{\mathbf{a}, \mathbf{b}\}$ and $\{\mathbf{e}_+, \mathbf{e}_-\}$ throughout the evolution. Of course, since $|A\rangle$ and $|B\rangle$ are orthogonal, we have that \mathbf{a} and \mathbf{b} are antiparallel (i.e., $\mathbf{a} \cdot \mathbf{b} = -1$). In the nonstationary time suboptimal evolution, instead, we typically have $\Delta E = \Delta E(t) < \Delta E_{\max}$, $|\langle E_+(t) | A \rangle|^2 \neq 1/2 \neq |\langle E_-(t) | A \rangle|^2$, $\mathbf{a} \cdot \mathbf{e}_+(t) \neq 0 \neq \mathbf{a} \cdot \mathbf{e}_-(t)$, and the path length of the actual dynamical trajectory is longer than the length of the geodesic path (i.e., $s > s_{\text{geo}}$). From a geometric standpoint, there is typically an absence of orthogonality between the Bloch vectors $\{\mathbf{a}, \mathbf{b}\}$ and the Bloch vectors $\{\mathbf{e}_+, \mathbf{e}_-\}$ throughout the quantum evolution. In fact, the generation of time suboptimal evolutions between orthogonal states in a two-dimensional space is quite feasible with time-dependent Hamiltonians, as it allows for a deviation from the orthogonality between $\{\mathbf{a}, \mathbf{b}\}$ and $\{\mathbf{e}_+, \mathbf{e}_-\}$. In conclusion, the symmetric arrangement that presents itself through the local (i.e., instantaneous) orthogonality between the Bloch vector $\mathbf{a}(t)$ with $0 \leq t \leq t_{\text{final}}$ and the Bloch eigenvectors $\{\mathbf{e}_+, \mathbf{e}_-\}$ prevents the emergence of dynamical paths with lengths other than π when evolving with a constant Hamiltonian between orthogonal states within a two-dimensional subspace of the larger Hilbert space. Considerations regarding optimal stationary and suboptimal nonstationary Hamiltonian evolutions, focusing on path lengths, energy uncertainties, probability amplitudes, and configurations of the Bloch vector appear in Table I.

We are now prepared to offer physical insights into how one can avert analog quantum search failures by drawing comparisons with occurrences in standard quantum evolutions between specified initial and final states.

V. ESCAPING ANALOG QUANTUM SEARCH FAILURES

In this section, we explore the concept of symmetry to pinpoint the source of failures in continuous time quantum search schemes involving orthogonal source and target states. Additionally, we propose methods to eliminate these

failures and, crucially, we establish an analogy with the failures observed in symmetric configurations that define time-optimal evolutions between orthogonal states governed by a stationary Hamiltonian.

A. Time-independent setting

The optimal time evolution between known initial and final states $|A\rangle$ and $|B\rangle$, respectively, is a distinct problem from that addressed in continuous-time quantum searching. In the latter scenario, the search is conducted from a known source state $|s\rangle$ to an unknown target state $|w\rangle$. Specifically, because the target state remains unknown, the modulus of the quantum overlap $|\langle s|w\rangle|$ between the source and target states is also indeterminate. However, these two quantum-mechanical processes possess a shared key feature. When both processes are defined by stationary Hamiltonians, and evolutions take place within the two-dimensional subspaces formed by the orthogonal sets of states $\{|A\rangle, |B\rangle\}$ or $\{|s\rangle, |w\rangle\}$, the inability to surpass the time-optimality of quantum evolutions is linked to the shortcomings of analog quantum search methods. More precisely, the inadequacy of H_{FG} in Eq. (1) is reflected in the asymptotically extended duration of the search scheme, as indicated by t_{FG} in Eq. (3). Notably, the inadequacy associated with H_{Fenner} in Eq. (4) is not apparent, as we observe that Fenner's Hamiltonian is constructed in a way that inherently prevents orthogonality between the source and target states. Indeed, we can substantiate this assertion by observing that H_{Fenner} in Eq. (4) represents a specific instance of H_{opt} in Eq. (11). To confirm this assertion, it suffices to set $|\langle A|B\rangle| = x$ and note that ΔE_{Fenner} simplifies to $\Delta E_{\text{Fenner}}(x) \stackrel{\text{def}}{=} 2xE\sqrt{1-x^2}$. Furthermore, while both H_{FG} and H_{Fenner} are optimal from the perspective of quantum search (in the sense that $t_{\text{FG}} \approx t_{\text{Fenner}} \propto \sqrt{N}$, with \sqrt{N} being the defining characteristic of Grover's algorithm quadratic speedup), only H_{Fenner} is genuinely time-optimal, as evidenced by $t_{\text{Fenner}} = t_{\text{opt}}^{\text{H}_{\text{Fenner}}}(x, E)$ (in contrast, $t_{\text{FG}} > t_{\text{opt}}^{\text{H}_{\text{FG}}}(x, E)$).

B. Time-dependent setting

To avoid failures in continuous-time quantum search between orthogonal source and target states, inspired by the approach of employing time-dependent Hamiltonians to create suboptimal evolutions between orthogonal states in two-dimensional subspaces, one might also explore time-dependent quantum search Hamiltonians [2, 14, 15, 19]. In this context, it is particularly crucial to highlight the principles of quantum search through local adiabatic [15] (or, alternatively, nonadiabatic [19]) evolutions. Within the framework of local adiabatic processes, it is observed that by adjusting the evolution rate of the Hamiltonian to ensure adiabatic evolution throughout each infinitesimal time interval, the total running time becomes proportional to \sqrt{N} . Notably, proper working of adiabatic quantum search Hamiltonians necessitate a nonvanishing minimum energy gap, which is defined as the smallest value of the energy difference between the two lowest instantaneous energy levels of the Hamiltonian, calculated over the temporal duration of the search. For instance, based on the research conducted by Roland and Cerf in Ref.[15], the local adiabatic search Hamiltonian is characterized as

$$H_{\text{RC}}(t) \stackrel{\text{def}}{=} \left(1 - \frac{t}{T}\right)H_s + \frac{t}{T}H_w = \tilde{H}(\xi) = (1 - \xi)H_s + \xi H_w, \quad (54)$$

with $0 \leq \xi \leq 1$, $H_s \stackrel{\text{def}}{=} \mathbf{1} + |s\rangle\langle s|$, $H_w \stackrel{\text{def}}{=} \mathbf{1} + |w\rangle\langle w|$ and, finally $|s\rangle = \left(1/\sqrt{N}\right) \sum_i |i\rangle$ with $\langle i|j\rangle = \delta_{ij}$ for any $1 \leq i, j \leq N$. A symmetric scenario occurs, for instance, when H_s and H_w in the decomposition of $\tilde{H}(\xi)$ are diagonal in the same basis. In this case, the energy levels $E_0(\xi)$ and $E_1(\xi)$ (with $E_0(\xi) \leq E_1(\xi) \leq \dots \leq E_{N-1}(\xi)$) of the Hamiltonian cross and, therefore, the minimum gap defined as $g_{\text{min}} \stackrel{\text{def}}{=} \min_{0 \leq \xi \leq 1} [E_1(\xi) - E_0(\xi)]$ vanishes [14]. This, in turn, leads to the failure of the searching scheme. In Fig. 3, we depict this fact. Interestingly, the issues with orthogonal states can also propagate to searching schemes specified by time-dependent Hamiltonians. For example, if one considers $\tilde{H}(\xi)$ in Eq. (54), problems emerge when $|s\rangle \stackrel{\text{def}}{=} |0\rangle$ and $|w\rangle \stackrel{\text{def}}{=} |1\rangle \in \{|0\rangle, |1\rangle\}$. Indeed, in this case $\tilde{H}(\xi)$ commutes with σ_z for any s and there is a level crossing that makes g_{min} equal to zero for some ξ . A similar situation arises when $|s\rangle \stackrel{\text{def}}{=} [|0\rangle + |1\rangle]/\sqrt{2}$ and $|w\rangle \stackrel{\text{def}}{=} [|0\rangle - |1\rangle]/\sqrt{2} \notin \{|0\rangle, |1\rangle\}$. Indeed, in this case $\tilde{H}(\xi)$ commutes with σ_x for any s and there exists a level crossing that causes g_{min} to vanish for some ξ . Therefore, because of the existence of a symmetry, the search scheme fails to work. More broadly, it can be noted that $\tilde{H}(\xi)$ in Eq. (54) satisfies the condition $[H_s, H_w] = 0$ when $\langle s|w\rangle = \langle w|s\rangle = 0$. Consequently, when the source and target states are orthogonal, it follows that $[\tilde{H}, H_s] = [\tilde{H}, H_w] = 0$. Once more, symmetries may result in search failures.

What is the role played by symmetry in the failure of quantum searching schemes? How is it related to the inability of transitioning between orthogonal states with a constant Hamiltonian in a sub-optimal time fashion? We

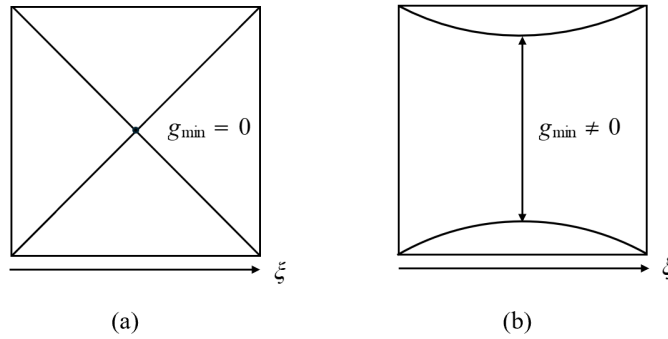


FIG. 3: In (a), there is a sketch of the two eigenvalues ξ and $1 - \xi$ of the time-dependent Hamiltonian $\tilde{H}(\xi) \stackrel{\text{def}}{=} (1 - \xi) [\mathbf{1} + |s\rangle \langle s|] + \xi [\mathbf{1} + |w\rangle \langle w|]$ when $|s\rangle \stackrel{\text{def}}{=} |0\rangle$, $|w\rangle \stackrel{\text{def}}{=} |1\rangle$, $\langle s | w \rangle = 0$, and the reduced time ξ being such that $0 \leq \xi \leq 1$. In this case, $\mathbf{1} + |s\rangle \langle s|$ and $\mathbf{1} + |w\rangle \langle w|$ are diagonal in the same basis, the eigenvalues cross and, therefore, $g_{\min} = 0$. In (b), there is a sketch of the two eigenvalues $(1 + \sqrt{(1 - \xi)^2 + \xi^2})/2$ and $(1 - \sqrt{(1 - \xi)^2 + \xi^2})/2$ of the time-dependent Hamiltonian $\tilde{H}(\xi) \stackrel{\text{def}}{=} (1 - \xi) [\mathbf{1} + |s\rangle \langle s|] + \xi [\mathbf{1} + |w\rangle \langle w|]$ when $|s\rangle \stackrel{\text{def}}{=} |0\rangle$, $|w\rangle \stackrel{\text{def}}{=} [|0\rangle + |1\rangle]/2$, $\langle s | w \rangle \neq 0$, and $0 \leq \xi \leq 1$. In this case, $\mathbf{1} + |s\rangle \langle s|$ and $\mathbf{1} + |w\rangle \langle w|$ are not diagonal in the same basis, the eigenvalues do not cross and, therefore, the minimum energy gap does not vanish since $g_{\min} \neq 0$.

recall that when the Hamiltonian of a system commutes with an operator, there is a symmetry in the system. We have that: i) The dynamics of the system is invariant under transformations generated by the operator; ii) The observable corresponding to the non-explicitly time-dependent operator is conserved in time; iii) The Hamiltonian and the operator share a common set of eigenstates, so they can be simultaneously diagonalized. For example, if $[\mathbf{H}, \sigma_z] = 0$, the system is symmetric under spin rotations about the z -axis and, in addition, the z -component of the spin is conserved.

The presence of a symmetry leads to conserved quantities and degeneracies. These, in turn, make it more likely that energy levels will cross as system parameters are varied. For example, consider a two-level Hamiltonian depending on a parameter $\lambda \in \mathbb{R}_+$ given by

$$\mathbf{H}(\lambda) \stackrel{\text{def}}{=} \begin{pmatrix} \lambda & \delta \\ \delta & -\lambda \end{pmatrix}. \quad (55)$$

If $\delta \neq 0$, the off-diagonal coupling causes level repulsion (i.e., no crossing). If $\delta = 0$, σ_z becomes a symmetry of the system and the energy levels cross at $\lambda = 0$. Therefore, one can conclude that level crossing generally requires decoupling, which is naturally provided by a symmetry. These factors assist in elucidating the function of symmetry in the breakdown of quantum search strategies. In particular, one expects that coupling terms in the search Hamiltonian can help in removing the failures. Indeed, consider search Hamiltonians of the form $\mathbf{H}(t) \stackrel{\text{def}}{=} [1 - s(t)] \mathbf{H}_0 + s(t) \mathbf{H}_f$ with $s(t) \in [0, 1]$, $\mathbf{H}_0 \stackrel{\text{def}}{=} -|\psi_0\rangle \langle \psi_0|$, $\mathbf{H}_f \stackrel{\text{def}}{=} -|\psi_f\rangle \langle \psi_f|$, and $\langle \psi_0 | \psi_f \rangle = 0$, the search fails for two reasons. First, the failure occurs because there is no overlap (i.e., $\langle \psi_f | \mathbf{H} | \psi_0 \rangle = 0$) to allow a direct transition via the interpolating Hamiltonian \mathbf{H} . Second, the failure occurs because the minimum energy gap vanishes (level crossing) in the presence of symmetry specified by the commutation relations $[\mathbf{H}(t), \mathbf{H}_0] = 0$ and $[\mathbf{H}(t), \mathbf{H}_f] = 0$ for any t . For example, setting $|\psi_0\rangle = |0\rangle$ and $|\psi_f\rangle = |1\rangle$, the energy gap is zero at $s = 1/2$. The failure can be fixed by introducing a coupling term like $\mathbf{H}_{\text{coupling}} \stackrel{\text{def}}{=} \gamma (|\psi_0\rangle \langle \psi_f| + |\psi_f\rangle \langle \psi_0|)$ with $\gamma > 0$ (or, alternatively, designing the search Hamiltonian to act in a larger subspace). Indeed, considering the Hamiltonian $\mathbf{H}(t) \stackrel{\text{def}}{=} -(1 - s)|0\rangle \langle 0| - s|1\rangle \langle 1| - \gamma(|0\rangle \langle 1| + |1\rangle \langle 0|)$, the energy gap becomes $\Delta(s) \stackrel{\text{def}}{=} 2\sqrt{(s - 1/2)^2 + \gamma^2}$. Therefore, the minimum energy gap reduces to $\Delta_{\min} = 2\gamma > 0$ at $s = 1/2$. Thus, the search can succeed in finite time. In general, the analog search Hamiltonian does not need to be optimal to work, it just needs to ensure non-zero coupling between the source and target states. If the coupling is weak, the runtime becomes large. However, the search still succeeds. A tabular summary detailing the causes of the failure of both the analyzed stationary and nonstationary search Hamiltonians when the source and target states are orthogonal is presented in Table II.

In conclusion, drawing from our insights, we determine that in order to prevent the failure of search algorithms, whether they involve constant or nonconstant Hamiltonians, it is essential to steer clear of highly symmetric configurations. Intuitively, this aligns with the understanding that when one proposes a solution to a problem, it is rare

Search scheme	Search Hamiltonian	Search failure and orthogonality	Reason of failure
Farhi-Gutmann	Stationary	Yes	Infinite search time
Fenner	Stationary	Yes	Scenario excluded by construction
Roland-Cerf	Nonstationary	Yes	Vanishing energy gap

TABLE II: Tabular overview outlining the reasons for the failure of both the examined stationary and nonstationary search Hamiltonians when the source and target states are orthogonal.

to achieve the ideal solution on the first try, and variations from the optimal solution are to be expected during this preliminary phase.

From our conversation regarding failures in quantum searching, a question arises quite naturally. In the scenario of standard Hamiltonian evolutions between specified initial and final orthogonal states, what symmetry exists within the system? What is the symmetry operator that commutes with the Hamiltonian? It is interesting to point out that in quantum mechanics, degeneracies arise from inherent symmetry and are removed when that symmetry is disrupted. For instance, when analyzing a quantum-mechanical particle confined in a box, the degeneracy exists due to the symmetry that is established when a general rectangular box is transformed into a cube [40]. Subsequently, the degeneracy is eliminated when the symmetry is compromised by altering the lengths of the sides. When focusing on qubit dynamics between orthogonal states with a constant Hamiltonian, from a group-theoretic perspective, it can be stated that there exists a discrete antipodal symmetry of the projective Hilbert space governed by $SU(2; \mathbb{C})$ dynamics defined by stationary Hamiltonians. Specifically, the antipodal \mathbb{Z}_2 inversion symmetry of the Bloch sphere is present (or absent) when considering stationary Hamiltonian evolutions between orthogonal (or nonorthogonal) states. Here, \mathbb{Z}_2 denotes the cyclic group of order 2 formed by two elements, the identity e and the involution g with $g^2 = e$. This antipodal symmetry is expressed by linking the initial and final states through the inversion map $g : \mathbf{a} \rightarrow -\mathbf{a}$, which effectively flips each Bloch vector \mathbf{a} through the origin. In scenarios involving orthogonal states, the evolution maintains symmetry concerning the inversion about the sphere's center. Conversely, when the evolution occurs between nonorthogonal states, this symmetry is forfeited, resulting in a diminished constraint on the dynamics. In the orthogonal scenario, since the states are interconnected by inversion symmetry, this symmetry imposes a constraint: the only constant Hamiltonian evolution that can precisely map one state to another must adhere to that symmetry. Generally, \mathbb{Z}_2 inversions are implemented through unitary involutions, which are inversion operators S satisfying $S^2 = \mathbf{1}$, $S|A\rangle = |B\rangle$, $S|B\rangle = |A\rangle$, and $[H, S] = 0$. For additional insights regarding group-theoretic arguments in physics, we suggest that interested readers refer to Ref. [41].

With these final comments, we are now prepared to present our summary of findings and concluding insights.

VI. FINAL REMARKS

The results outlined in this paper were influenced by two main factors. First, in the field of analog quantum searching that utilizes time-independent Hamiltonians, the search technique is ineffective when the source and target states are orthogonal. Second, with respect to optimal-time evolutions, it is impossible to evolve in a two-dimensional space in a time suboptimal manner between two orthogonal states while employing a stationary Hamiltonian. Driven by these two constraints related to orthogonal states, this paper aimed to thoroughly examine these matters to enhance our theoretical comprehension of the shared principles that underpin both the achievements and shortcomings of analog quantum searches and time-optimal quantum evolutions, based on fundamental physical principles and symmetry considerations.

Our analysis shows that at the level of single-qubit dynamics generated by a time-independent Hamiltonian, evolution between orthogonal states is strongly constrained by symmetry. In particular, the dynamics preserves an antipodal inversion symmetry on the Bloch sphere: orthogonal states lie at opposite poles, and unitary evolution corresponds to a rotation that necessarily respects this geometric inversion symmetry. As a result, within this setting, there is no mechanism to break the symmetry in a way that would qualitatively alter the structure of the evolution. In the context of quantum search Hamiltonians, instead, we showed that the presence of continuous symmetries, such as rotational invariance, frequently gives rise to energy degeneracies and possible level crossings in the spectrum. Such degeneracies can obstruct controlled dynamical evolution, for example by preventing the opening of an energy gap that governs the runtime of the algorithm. By deliberately breaking certain symmetries- while preserving those essential to the computational task- one can lift degeneracies, avoid level crossings, and generate a finite spectral gap. This gap, in turn, ensures well-defined and finite search times. In this sense, symmetry is not merely a structural constraint but a resource that can either hinder or enable efficient quantum dynamics, depending on how it is engineered.

An outline of our principal discoveries is as follows:

- [i] We clarified that both H_{FG} (Eq. (1)) and H_{Fenner} (Eq. (4)) are optimal from the perspective of quantum search ((i.e., in terms of minimum number of oracle calls)). However, regarding time optimal evolution, H_{FG} is deemed suboptimal, while H_{Fenner} is optimal. Additionally, due to its time suboptimal nature, H_{FG} is ineffective for searches between orthogonal states. Conversely, H_{Fenner} has been demonstrated to be a time-optimal Hamiltonian (Eq. (11)) suitable for nonorthogonal states. Consequently, it was inherently designed not to be utilized for searches between orthogonal states (Table II).
- [ii] We employed energy arguments (Eq. (25)) to demonstrate that it is not feasible to unitarily evolve between orthogonal states using a constant Hamiltonian within the two-dimensional subspace defined by the initial and final states in a manner that is suboptimal in time.
- [iii] From a geometric perspective, we illustrated (Fig. 1 and Table I) that the evolution between orthogonal states governed by a constant Hamiltonian is defined by a symmetry determined by the instantaneous orthogonality conditions between the Bloch vector $\mathbf{a}(t)$ of the evolving state vector $|\psi(t)\rangle$ and the Bloch vectors of the energy eigenstates \mathbf{e}_{\pm} . These conditions arise from the constancy of the probability amplitudes $|\langle E_{\pm}|\psi(t)\rangle|^2 = 1/2$ and are further characterized by the relation $\mathbf{a}(t) \cdot \mathbf{e}_{\pm} = 0$, at any given instant t .
- [iv] We investigated a time suboptimal evolution between orthogonal states utilizing a time-dependent Hamiltonian. We explicitly confirmed that the violation of the symmetry condition $\mathbf{a}(t) \cdot \mathbf{e}_{\pm}(t) \neq 0$ permits a deviation from time optimality, with the probability amplitude $|\langle E_{\pm}(t)|\psi(t)\rangle|^2$ typically differing from $1/2$ (Eqs. (50), (51), (52), (53) and Fig. 2).
- [v] We connected the shortcomings of adiabatic quantum searches (Eq. (54)) between orthogonal states, attributed to the symmetries of the time-dependent search Hamiltonian that lead to a vanishing minimum energy gap, with the failures observed with the transition between orthogonal states with a constant Hamiltonian in a sub-optimal time fashion.

The inability to transition between orthogonal states with a constant Hamiltonian in a sub-optimal time is significantly related to the failure of analog quantum search when the source and target states are orthogonal and not coupled by the Hamiltonian. In both cases, the root of the failure is the presence of an underlying symmetry of the system. These underlying symmetries can be geometrically grasped by means of Figs. 1 and 3. In Fig. 1, the geometry of Bloch vectors for a time optimal evolution (Fig. 1, (a); time optimal) between orthogonal states displays a higher degree of symmetry compared with the geometry of Bloch vectors for a time sub-optimal evolution (Fig. 1, (b); time sub-optimal) between the same orthogonal initial and final states. Similarly, Fig. 3 hints to the fact that the square with diagonals (Fig. 3, (a); crossing) exhibits a higher degree of symmetry than the square with two non-intersecting curves (Fig. 3, (b); no crossing).

Our analysis in this paper centers on both discrete and continuous symmetries of quantum systems. In the discrete symmetry setting, we focused on qubit dynamics between orthogonal states with a constant Hamiltonian. In this case, to experimentally detect the presence of antipodal \mathbb{Z}_2 inversion symmetry in a system with Hamiltonian $H \stackrel{\text{def}}{=} \mathbf{h} \cdot \boldsymbol{\sigma}$, one can proceed as follows. Pick the axis \mathbf{n} of the putative π -flip symmetry operator $S \stackrel{\text{def}}{=} \mathbf{n} \cdot \boldsymbol{\sigma}$ with $[H, e^{-i\frac{\pi}{2}S}] = 2(\mathbf{h} \times \mathbf{n}) \cdot \boldsymbol{\sigma}$, where $U_{\pi}(\mathbf{n}) \stackrel{\text{def}}{=} e^{-i\frac{\pi}{2}S} = e^{-i\frac{\pi}{2}\mathbf{n} \cdot \boldsymbol{\sigma}}$ is a π rotation about the unit vector \mathbf{n} . Prepare the qubit in an eigenstate of S and let it evolve under the Hamiltonian H . If the \mathbb{Z}_2 symmetry is indeed present, the expectation value of S remains constant over time. In this scenario, $\langle S(0) \rangle = \langle S(t) \rangle$ with \mathbf{h} and \mathbf{n} aligned. Conversely, if the \mathbb{Z}_2 symmetry is absent, the expectation value of S will vary over time. In this case, $\langle S(0) \rangle \neq \langle S(t) \rangle$ with \mathbf{h} and \mathbf{n} not aligned. In the continuous symmetry setting, we focused on quantum search Hamiltonians. In this case, we essentially limited our attention to the invariance of the Hamiltonians under rotations by any angle θ around an arbitrary axis \mathbf{n} . Comparing discrete and continuous symmetry settings, \mathbb{Z}_2 is replaced by $U(1; \mathbb{C}) \stackrel{\text{def}}{=} \{e^{i\theta} : \theta \in [0, 2\pi)\}$ and, in particular, $e^{-i\frac{\theta}{2}\mathbf{n} \cdot \boldsymbol{\sigma}}$ replaces $e^{-i\frac{\pi}{2}\mathbf{n} \cdot \boldsymbol{\sigma}}$. For instance, the commutation relation $[H, \sigma_z] = 0$ indicates the presence of an exact, continuous, unitary, global internal symmetry, corresponding to invariance under spin rotations about the z -axis. From an experimental perspective, we stress that such types of continuous symmetries are recognized indirectly via conserved observables, selection rules in spectroscopy, symmetry-protected degeneracies, and dynamics occurring within invariant subspaces [42]. A particularly effective diagnostic approach is the intentional breaking of symmetry: previously conserved quantities begin to vary, transitions that were once prohibited arise, and degeneracies split into avoided crossings. The robustness of these indicators in the face of parameter variations provides concrete evidence of the underlying symmetry. For example, to verify that H commutes with an operator \mathcal{O} , one can prepare

quantum states with different initial values of $\langle \mathcal{O}(0) \rangle$, let the system evolve, and measure $\langle \mathcal{O}(t) \rangle$ at later times. If the symmetry is present, $\langle \mathcal{O}(t) \rangle$ remains constant and equal to $\langle \mathcal{O}(0) \rangle$. Alternatively, using controlled symmetry breaking procedures, one can introduce a small, tunable perturbation that explicitly breaks the suspected symmetry (for example, adding a transverse field if $[\mathcal{H}, \sigma_z] = 0$). By observing how the spectrum and dynamics respond, one can determine the presence of the original symmetry. If conserved quantities begin to evolve, or if degeneracies split into avoided crossings or previously forbidden transitions become allowed, the underlying symmetry can be identified. For more details on theoretical and experimental aspects of discrete and continuous symmetries beyond Schrödinger's evolutions and quantum search Hamiltonians, we recommend consulting Ref. [42].

Summing up, symmetry can be utilized to elucidate the shortcomings of analog quantum search schemes, whether stationary or nonstationary, in the context of orthogonal (known) source and (unknown) target states. Furthermore, symmetry arguments can be employed to demonstrate the impossibility of creating suboptimal time stationary Hamiltonian evolutions between specified initial and final orthogonal quantum states. In the first instance, symmetry results in energy level crossing, which consequently leads to asymptotically prolonged search times, rendering the search ineffective. Conversely, in the latter scenario, the existence of a discrete antipodal symmetry prevents the evolution from deviating from the optimal time trajectory defined by a geodesic path on the Bloch sphere that connects the initial and final states.

We remark that the growing fascination with the significance of symmetries and conserved quantities in quantum control theory [43] and quantum search [44, 45] renders our research particularly appealing to scientists who are tackling these challenges (i.e., control and search) from a group-theoretic perspective. Our analysis centered on eliminating failures (in both search and control) within two-dimensional subspaces of the complete Hilbert space. However, in the realm of time-optimal evolutions, it is possible to explore the construction of stationary Hamiltonians that dictate the evolution between two orthogonal states in higher-dimensional subspaces in a less than optimal time manner. Furthermore, regarding quantum search between orthogonal source and target states, one might consider the potential for failure reduction by increasing the dimensionality of the search space [46, 47], albeit at the cost of optimal query complexity. We will defer these discussions to future scientific endeavors.

ACKNOWLEDGMENTS

C.C. is grateful to the Griffiss Institute (Rome-NY) and to the United States Air Force Research Laboratory (AFRL) Visiting Faculty Research Program (VFRP) for providing support for this work. J.S. gratefully acknowledges support from the AFRL. The authors express their gratitude for the enlightening discussions held with P. M. Alsing. Any opinions, findings and conclusions or recommendations expressed in this material are those of the authors and do not necessarily reflect the views of the AFRL. The authors thank the three anonymous referees for very useful comments leading to an improved version of this manuscript.

-
- [1] E. Farhi and S. Gutmann, *An analog analogue of a digital quantum computation*, Phys. Rev. **A57**, 2403 (1998).
 - [2] C. Cafaro and P. M. Alsing, *Continuous-time quantum search and time-dependent two-level quantum systems*, Int. J. Quantum Information **17**, 1950025 (2019).
 - [3] S. Gassner, C. Cafaro, and S. Capozziello, *Transition probabilities in generalized quantum search Hamiltonian evolutions*, Int. J. Geom. Meth. Mod. Phys. **17**, 2050006 (2020).
 - [4] A. Mostafazadeh, *Hamiltonians generating optimal-speed evolutions*, Phys. Rev. **A79**, 014101 (2009).
 - [5] C. M. Bender, D. C. Brody, H. F. Jones, and B. K. Meister, *Faster than Hermitian quantum mechanics*, Phys. Rev. Lett. **98**, 040403 (2007).
 - [6] C. Cafaro and P. M. Alsing, *Qubit geodesics on the Bloch sphere from optimal-speed Hamiltonian evolutions*, Class. Quantum Grav. **40**, 115005 (2023).
 - [7] D. C. Brody, *Elementary derivation for passage times*, J. Phys.: Math. Gen. **36**, 5587 (2003).
 - [8] L. K. Grover, *Quantum mechanics helps in searching for a needle in a haystack*, Phys. Rev. Lett. **79**, 325 (1997).
 - [9] L. K. Grover, *Fixed-point quantum search*, Phys. Rev. Lett. **95**, 150501 (2005).
 - [10] C. Zalka, *Grover's quantum searching algorithm is optimal*, Phys. Rev. **A60**, 2746 (1999).
 - [11] A. Miyake and M. Wadati, *Geometric strategy for the optimal quantum search*, Phys. Rev. **A64**, 042317 (2001).
 - [12] C. Cafaro, *Geometric algebra and information geometry for quantum computational software*, Physica **A470**, 154 (2017).
 - [13] J. Bae and Y. Kwon, *Generalized quantum search Hamiltonians*, Phys. Rev. **A66**, 012314 (2002).
 - [14] E. Farhi, J. Goldstone, S. Gutmann, and M. Sipser, *Quantum computation by adiabatic evolution*, arXiv:quant-ph/0001106 (2000).
 - [15] J. Roland and N. J. Cerf, *Quantum search by local adiabatic evolution*, Phys. Rev. **A65**, 042308 (2002).

-
- [16] K.-P. Marzlin and B. C. Sanders, *Inconsistency in the application of the adiabatic theorem*, Phys. Rev. Lett. **93**, 160408 (2004).
- [17] D. M. Tong, K. Singh, L. C. Kwek, and C. H. Oh, *Quantitative conditions do not guarantee the validity of the adiabatic approximation*, Phys. Rev. Lett. **95**, 110407 (2005).
- [18] M. Andrecut and M. K. Ali, *The adiabatic analogue of the Margolus-Levitin theorem*, J. Phys. A: Math. Gen. **37**, L157 (2004).
- [19] A. Perez and A. Romanelli, *Nonadiabatic quantum search algorithms*, Phys. Rev. **A76**, 052318 (2007).
- [20] C. Cafaro and S. Mancini, *An information geometric viewpoint of algorithms in quantum computing*, in Bayesian Inference and Maximum Entropy Methods in Science and Engineering, AIP Conf. Proc. **1443**, 374 (2012).
- [21] C. Cafaro and S. Mancini, *On Grover's search algorithm from a quantum information geometry viewpoint*, Physica **A391**, 1610 (2012).
- [22] J. Anandan and Y. Aharonov, *Geometry of quantum evolution*, Phys. Rev. Lett. **65**, 1697 (1990).
- [23] G. A. Hamilton and B. K. Clark, *Quantifying unitary flow efficiency and entanglement for many-body localization*, Phys. Rev. **B107**, 064203 (2023).
- [24] C. Cafaro, S. Ray, and P. M. Alsing, *Optimal-speed unitary quantum time evolutions and propagation of light with maximal degree of coherence*, Phys. Rev. **A105**, 052425 (2022).
- [25] E. Wolf, *Coherence properties of partially polarized electromagnetic radiation*, Il Nuovo Cimento **13**, 1180 (1959).
- [26] E. Wolf, *Introduction to the Theory of Coherence and Polarization of Light*, Cambridge University Press (2007).
- [27] L. Rossetti, C. Cafaro, and N. Bahreyni, *Constructions of optimal-speed quantum evolutions: A comparative study*, Physica Scripta **99**, 095121 (2024).
- [28] S. Haywood, *Symmetries and Conservation Laws in Particle Physics*, Imperial College Press (2010).
- [29] D. Lu et al., *Chiral quantum walks*, Phys. Rev. **A93**, 042302 (2016).
- [30] T. Chen, B. Wang, and X. Zhang, *Controlling probability transfer in the discrete-time quantum walk by modulating the symmetries*, New J. Phys. **19**, 113049 (2017).
- [31] D. Manzano and P. I. Hurtado, *Harnessing symmetry to control quantum transport*, Adv. Phys. **67**, 1 (2018).
- [32] A. Bottarelli et al., *Symmetry-enhanced counteradiabatic quantum algorithms for qudits*, Phys. Rev. Research **7**, 043030 (2025).
- [33] S. Fenner, *An intuitive Hamiltonian for quantum search*, arXiv:quant-ph/0004091 (2000).
- [34] C. Cafaro, E. Clements, and A. Alanazi, *Aspects of complexity in quantum evolutions on the Bloch sphere*, Eur. Phys. J. Plus **140**, 349 (2025).
- [35] R. Uzdin, U. Günther, S. Rahav, and N. Moiseyev, *Time-dependent Hamiltonians with 100% evolution speed efficiency*, J. Phys. A: Math. Theor. **45**, 415304 (2012).
- [36] C. Cafaro, S. Ray, and P. M. Alsing, *Geometric aspects of analog quantum search evolutions*, Phys. Rev. **A102**, 052607 (2020).
- [37] L. Rossetti, C. Cafaro, and P. M. Alsing, *Deviations from geodesic evolutions and energy waste on the Bloch sphere*, Phys. Rev. **A111**, 022441 (2025).
- [38] R. P. Feynman, F. Vernon, and R. W. Hellwarth, *Geometrical representation of the Schrödinger equation for solving maser problems*, J. Appl. Phys. **28**, 49 (1957).
- [39] C. Cafaro, L. Rossetti, and P. M. Alsing, *Curvature of quantum evolutions for qubits in time-dependent magnetic fields*, Phys. Rev. **A111**, 012408 (2025).
- [40] D. A. McQuarrie, *Quantum Chemistry*, University Science Books (2008).
- [41] M. Hamermesh, *Group Theory and Its Application to Physical Problems*, Dover Publications (1989).
- [42] D. C. Harris and M. D. Bertolucci, *Symmetry and Spectroscopy*, Dover Publications, Inc., New York (1989).
- [43] F. Albertini and D. D'Alessandro, *On symmetries in time optimal control, sub-Riemannian geometries, and the K-P problem*, J. Dyn. Control Sys. **24**, 13 (2018).
- [44] Y. Wang and S. Wu, *Role of symmetry in quantum search via continuous-time quantum walk*, SPIN **11**, 2140002 (2021).
- [45] D. A. Meyer and T. G. Wang, *Conserved quantities in linear and nonlinear quantum search*, Quantum Inf. Comput. **25**, 315 (2025).
- [46] R. A. Gutoiu, A. Tanasescu, and P. G. Popescu, *Simple exact quantum search*, Quantum Inf. Process. **23**, 356 (2024).
- [47] S.-M. Ye and Y.-L. Wang, *Deterministic quantum partial search for target states with proportion 1/16*, Phys. Lett. **A537**, 130325 (2025).
- [48] M. A. Nielsen and I. L. Chuang, *Quantum Computation and Quantum Information*, Cambridge University Press (2010).
- [49] J. P. Provost and G. Vallee, *Riemannian structure on manifolds of quantum states*, Commun. Math. Phys. **76**, 289 (1980).
- [50] S. Braunstein and C. M. Caves, *Statistical distance and the geometry of quantum states*, Phys. Rev. Lett. **72**, 3439 (1994).

Appendix A: Derivation of Eq. (5)

In this appendix, we calculate the transition probability $\mathcal{P}_{\text{Fenner}}(t)$ in Eq. (5).

Consider the Hamiltonian $H_{\text{Fenner}} \stackrel{\text{def}}{=} 2iEx(|w\rangle\langle s| - |s\rangle\langle w|)$ with the source state $|s\rangle = x|w\rangle + \sqrt{1-x^2}|r\rangle$ in the orthonormal basis $\{|w\rangle, |r\rangle\}$. Then, the matrix representation of H_{Fenner} in the basis $\{|w\rangle, |r\rangle\}$ is given by

$$[H_{\text{Fenner}}]_{\{|w\rangle, |r\rangle\}} \stackrel{\text{def}}{=} \begin{pmatrix} \langle w|H_{\text{Fenner}}|w\rangle & \langle w|H_{\text{Fenner}}|r\rangle \\ \langle r|H_{\text{Fenner}}|w\rangle & \langle r|H_{\text{Fenner}}|r\rangle \end{pmatrix} = \begin{pmatrix} 0 & 2iEx\sqrt{1-x^2} \\ -2iEx\sqrt{1-x^2} & 0 \end{pmatrix}. \quad (\text{A1})$$

From a simple calculation, we get that the energy eigenvalues of $[H_{\text{Fenner}}]_{\{|w\rangle, |r\rangle\}}$ are $E_1 \stackrel{\text{def}}{=} 2Ex\sqrt{1-x^2}$ and $E_2 \stackrel{\text{def}}{=} -2Ex\sqrt{1-x^2}$. A corresponding set of orthonormal eigenstates is given by

$$|E_1\rangle \stackrel{\text{def}}{=} \frac{|w\rangle - i|r\rangle}{\sqrt{2}}, \text{ and } |E_2\rangle \stackrel{\text{def}}{=} \frac{|w\rangle + i|r\rangle}{\sqrt{2}}, \quad (\text{A2})$$

respectively. Using Eq. (A2), we can recast the source state, the target state, and the Hamiltonian H_{Fenner} in terms of the eigenstates $|E_1\rangle$ and $|E_2\rangle$. We have,

$$|s\rangle = \frac{x + i\sqrt{1-x^2}}{\sqrt{2}}|E_1\rangle + \frac{x - i\sqrt{1-x^2}}{\sqrt{2}}|E_2\rangle, \quad |w\rangle = \frac{|E_1\rangle + |E_2\rangle}{\sqrt{2}}, \quad (\text{A3})$$

and, finally,

$$H_{\text{Fenner}} = E_1|E_1\rangle\langle E_1| + E_2|E_2\rangle\langle E_2|. \quad (\text{A4})$$

Finally, making use of Eqs. (A3) and (A4), the transition probability $\mathcal{P}_{\text{Fenner}}(t) \stackrel{\text{def}}{=} \left| \langle w | e^{-\frac{i}{\hbar}H_{\text{Fenner}}t} | s \rangle \right|^2$ becomes

$$\mathcal{P}_{\text{Fenner}}(t) = \left| x \cos\left(2x\sqrt{1-x^2}\frac{Et}{\hbar}\right) + \sqrt{1-x^2} \sin\left(2x\sqrt{1-x^2}\frac{Et}{\hbar}\right) \right|^2. \quad (\text{A5})$$

The calculation of $\mathcal{P}_{\text{Fenner}}(t)$ in Eq. (A5) ends our derivation.

Appendix B: Quantum search as quantum simulation

In this appendix, we explain how the time evolution sub-optimality of the Fahri-Gutmann search Hamiltonian $H_{\text{FG}} = E|w\rangle\langle w| + E|s\rangle\langle s|$ can be understood in geometric terms by re-deriving the search Hamiltonian from the point of view of quantum simulation. This statement was reported in the end of Section II.

Specifically, one needs to study in an explicit manner the action of a simulation step of time Δt specified by the unitary operator $U(t)$ given by

$$U(\Delta t) \stackrel{\text{def}}{=} e^{-i|s\rangle\langle s|\Delta t} e^{-i|w\rangle\langle w|\Delta t}, \quad (\text{B1})$$

where we set $E = 1 = \hbar$. To calculate $U(\Delta t)$ in Eq. (B1), we can focus on studying how one can express the sequential application of two rotations $\mathcal{R}_{\mathbf{n}_1}(\theta_1)$ and $\mathcal{R}_{\mathbf{n}_2}(\theta_2)$ on a single qubit in terms of a single rotation specified by $\mathcal{R}_{\mathbf{n}}(\theta)$. Formally, setting

$$e^{-i\frac{\theta_1}{2}\mathbf{n}_1\cdot\boldsymbol{\sigma}} e^{-i\frac{\theta_2}{2}\mathbf{n}_2\cdot\boldsymbol{\sigma}} = e^{-i\frac{\theta}{2}\mathbf{n}\cdot\boldsymbol{\sigma}}, \quad (\text{B2})$$

one needs to find the angle θ and the axis of rotation \mathbf{n} in Eq. (B2). We proceed as follows. Note that [48],

$$\begin{aligned} e^{-i\frac{\theta}{2}\mathbf{n}\cdot\boldsymbol{\sigma}} &= e^{-i\frac{\theta_1}{2}\mathbf{n}_1\cdot\boldsymbol{\sigma}} e^{-i\frac{\theta_2}{2}\mathbf{n}_2\cdot\boldsymbol{\sigma}} \\ &= \left[\cos\left(\frac{\theta_1}{2}\right) \mathbf{I} - i \sin\left(\frac{\theta_1}{2}\right) \mathbf{n}_1 \cdot \boldsymbol{\sigma} \right] \left[\cos\left(\frac{\theta_2}{2}\right) \mathbf{I} - i \sin\left(\frac{\theta_2}{2}\right) \mathbf{n}_2 \cdot \boldsymbol{\sigma} \right] \\ &= \cos\left(\frac{\theta_1}{2}\right) \cos\left(\frac{\theta_2}{2}\right) \mathbf{I} - i \cos\left(\frac{\theta_1}{2}\right) \sin\left(\frac{\theta_2}{2}\right) \mathbf{n}_2 \cdot \boldsymbol{\sigma} - i \sin\left(\frac{\theta_1}{2}\right) \cos\left(\frac{\theta_2}{2}\right) \mathbf{n}_1 \cdot \boldsymbol{\sigma} + \\ &\quad - \sin\left(\frac{\theta_1}{2}\right) \sin\left(\frac{\theta_2}{2}\right) (\mathbf{n}_1 \cdot \boldsymbol{\sigma})(\mathbf{n}_2 \cdot \boldsymbol{\sigma}). \end{aligned} \quad (\text{B3})$$

To simplify Eq. (B3), we use ordinary quantum-mechanical properties of Pauli matrices. We have,

$$\begin{aligned}
(\mathbf{n}_1 \cdot \boldsymbol{\sigma})(\mathbf{n}_2 \cdot \boldsymbol{\sigma}) &= (n_{1i}\sigma_i)(n_{2j}\sigma_j) \\
&= n_{1i}n_{2j}\sigma_i\sigma_j \\
&= n_{1i}n_{2j} \left(\frac{1}{2} [\sigma_i, \sigma_j] + \frac{1}{2} \{\sigma_i, \sigma_j\} \right) \\
&= n_{1i}n_{2j} \left(\frac{1}{2} 2i\varepsilon_{ijk}\sigma_k + \frac{1}{2} 2\delta_{ij} \right) \\
&= n_{1i}n_{2j}\delta_{ij} + i\varepsilon_{ijk}n_{1i}n_{2j}\sigma_k \\
&= (\mathbf{n}_1 \cdot \mathbf{n}_2) \mathbf{I} + i(\mathbf{n}_1 \times \mathbf{n}_2) \cdot \boldsymbol{\sigma},
\end{aligned} \tag{B4}$$

that is,

$$(\mathbf{n}_1 \cdot \boldsymbol{\sigma})(\mathbf{n}_2 \cdot \boldsymbol{\sigma}) = (\mathbf{n}_1 \cdot \mathbf{n}_2) \mathbf{I} + i(\mathbf{n}_1 \times \mathbf{n}_2) \cdot \boldsymbol{\sigma}. \tag{B5}$$

Therefore, substituting Eq. (B5) into Eq. (B3), we arrive at

$$\begin{aligned}
e^{-i\frac{\theta}{2}\mathbf{n}\cdot\boldsymbol{\sigma}} &= \cos\left(\frac{\theta_1}{2}\right)\cos\left(\frac{\theta_2}{2}\right)\mathbf{I} - i\cos\left(\frac{\theta_1}{2}\right)\sin\left(\frac{\theta_2}{2}\right)\mathbf{n}_2 \cdot \boldsymbol{\sigma} - i\sin\left(\frac{\theta_1}{2}\right)\cos\left(\frac{\theta_2}{2}\right)\mathbf{n}_1 \cdot \boldsymbol{\sigma} \\
&\quad - \sin\left(\frac{\theta_1}{2}\right)\sin\left(\frac{\theta_2}{2}\right)(\mathbf{n}_1 \cdot \mathbf{n}_2)\mathbf{I} - i\sin\left(\frac{\theta_1}{2}\right)\sin\left(\frac{\theta_2}{2}\right)(\mathbf{n}_1 \times \mathbf{n}_2) \cdot \boldsymbol{\sigma} \\
&= \left[\cos\left(\frac{\theta_1}{2}\right)\cos\left(\frac{\theta_2}{2}\right) - \sin\left(\frac{\theta_1}{2}\right)\sin\left(\frac{\theta_2}{2}\right)(\mathbf{n}_1 \cdot \mathbf{n}_2) \right] \mathbf{I} + \\
&\quad - i \left[\sin\left(\frac{\theta_1}{2}\right)\cos\left(\frac{\theta_2}{2}\right)\mathbf{n}_1 + \cos\left(\frac{\theta_1}{2}\right)\sin\left(\frac{\theta_2}{2}\right)\mathbf{n}_2 - \sin\left(\frac{\theta_1}{2}\right)\sin\left(\frac{\theta_2}{2}\right)(\mathbf{n}_2 \times \mathbf{n}_1) \right] \cdot \boldsymbol{\sigma} \\
&= \left[\cos\left(\frac{\theta}{2}\right)\mathbf{I} - i\sin\left(\frac{\theta}{2}\right)\mathbf{n} \cdot \boldsymbol{\sigma} \right],
\end{aligned} \tag{B6}$$

that is,

$$\begin{cases} \cos\left(\frac{\theta}{2}\right) = \cos\left(\frac{\theta_1}{2}\right)\cos\left(\frac{\theta_2}{2}\right) - \sin\left(\frac{\theta_1}{2}\right)\sin\left(\frac{\theta_2}{2}\right)(\mathbf{n}_1 \cdot \mathbf{n}_2), \\ \sin\left(\frac{\theta}{2}\right)\mathbf{n} = \sin\left(\frac{\theta_1}{2}\right)\cos\left(\frac{\theta_2}{2}\right)\mathbf{n}_1 + \cos\left(\frac{\theta_1}{2}\right)\sin\left(\frac{\theta_2}{2}\right)\mathbf{n}_2 - \sin\left(\frac{\theta_1}{2}\right)\sin\left(\frac{\theta_2}{2}\right)(\mathbf{n}_2 \times \mathbf{n}_1) \end{cases}. \tag{B7}$$

Finally, Eq. (B7) allows us to specify the rotation angle θ and the rotation axis \mathbf{n} in $\mathcal{R}_{\mathbf{n}}(\theta) = \mathcal{R}_{\mathbf{n}_1}(\theta_1)\mathcal{R}_{\mathbf{n}_2}(\theta_2)$.

Returning to the expression for $U(\Delta t)$ in Eq. (B1), let us set

$$|s\rangle\langle s| = \frac{\mathbf{I} + \mathbf{s} \cdot \boldsymbol{\sigma}}{2}, \text{ and } |w\rangle\langle w| = \frac{\mathbf{I} + \mathbf{w} \cdot \boldsymbol{\sigma}}{2}, \tag{B8}$$

where $\mathbf{s} \stackrel{\text{def}}{=} (2x\sqrt{1-x^2}, 0, 2x^2-1)$ and $\mathbf{w} \stackrel{\text{def}}{=} \hat{z} = (0, 0, 1)$ are unit vectors. Substituting Eq. (B8) into Eq. (B1), $U(\Delta t)$ becomes

$$\begin{aligned}
U(\Delta t) &= e^{-i|s\rangle\langle s|\Delta t} e^{-i|w\rangle\langle w|\Delta t} \\
&= e^{-i\frac{1+\mathbf{s}\cdot\boldsymbol{\sigma}}{2}\Delta t} e^{-i\frac{1+\mathbf{w}\cdot\boldsymbol{\sigma}}{2}\Delta t} \\
&= e^{-i\frac{1}{2}\Delta t} e^{-i\frac{\mathbf{s}\cdot\boldsymbol{\sigma}}{2}\Delta t} e^{-i\frac{1}{2}\Delta t} e^{-i\frac{\mathbf{w}\cdot\boldsymbol{\sigma}}{2}\Delta t} \\
&= e^{-i\Delta t} e^{-i\frac{\mathbf{s}\cdot\boldsymbol{\sigma}}{2}\Delta t} e^{-i\frac{\mathbf{w}\cdot\boldsymbol{\sigma}}{2}\Delta t} \\
&\approx e^{-i\frac{\mathbf{s}\cdot\boldsymbol{\sigma}}{2}\Delta t} e^{-i\frac{\mathbf{w}\cdot\boldsymbol{\sigma}}{2}\Delta t},
\end{aligned} \tag{B9}$$

where in the last step in Eq. (B9) we neglect the irrelevant global phase factor $e^{-i\Delta t}$. Now, we want to use Eq. (B7) to express $e^{-i\frac{\mathbf{s}\cdot\boldsymbol{\sigma}}{2}\Delta t} e^{-i\frac{\mathbf{w}\cdot\boldsymbol{\sigma}}{2}\Delta t}$ as $e^{-i\frac{\theta}{2}\mathbf{n}\cdot\boldsymbol{\sigma}}$. Using Eqs. (B7) and (B9), we find that \mathbf{n} and θ such that

$e^{-i\frac{\theta}{2}\mathbf{n}\cdot\boldsymbol{\sigma}} = e^{-i\frac{s}{2}\Delta t}e^{-i\frac{w}{2}\Delta t}$ satisfy the following two relations,

$$\begin{cases} \cos\left(\frac{\theta}{2}\right) = \cos^2\left(\frac{\Delta t}{2}\right) - \sin^2\left(\frac{\Delta t}{2}\right)\mathbf{s}\cdot\mathbf{w} \\ \sin\left(\frac{\theta}{2}\right)\mathbf{n} = \sin\left(\frac{\Delta t}{2}\right)\cos\left(\frac{\Delta t}{2}\right)(\mathbf{s}+\mathbf{w}) - \sin^2\left(\frac{\Delta t}{2}\right)\mathbf{w}\times\mathbf{s} \end{cases} \quad (\text{B10})$$

Therefore, from Eqs. (B9) and (B10), $U(\Delta t) \approx e^{-i\frac{s}{2}\Delta t}e^{-i\frac{w}{2}\Delta t}$ can be recast as

$$U(\Delta t) \approx \left[\cos^2\left(\frac{\Delta t}{2}\right) - \sin^2\left(\frac{\Delta t}{2}\right)\mathbf{s}\cdot\mathbf{w} \right] \mathbf{I} - 2i \sin\left(\frac{\Delta t}{2}\right) \left[\cos\left(\frac{\Delta t}{2}\right)\left(\frac{\mathbf{s}+\mathbf{w}}{2}\right) + \sin\left(\frac{\Delta t}{2}\right)\left(\frac{\mathbf{s}\times\mathbf{w}}{2}\right) \right] \cdot \boldsymbol{\sigma}. \quad (\text{B11})$$

The unnormalized axis of rotation that specifies $U(\Delta t)$ in Eq. (B11) is given by

$$\mathbf{r} \stackrel{\text{def}}{=} \cos\left(\frac{\Delta t}{2}\right)\left(\frac{\mathbf{s}+\mathbf{w}}{2}\right) + \sin\left(\frac{\Delta t}{2}\right)\left(\frac{\mathbf{s}\times\mathbf{w}}{2}\right), \quad (\text{B12})$$

with $\mathbf{r} = \|\mathbf{r}\| \hat{r} = (x\sqrt{1-x^2})\cos(\Delta t/2)$, $-x\sqrt{1-x^2}\sin(\Delta t/2)$, $x^2\cos(\Delta t/2)$. After some algebra with Eqs. (B10), (B11), and (B12), $U(\Delta t)$ can be finally expressed as

$$U(\Delta t) = \cos\left[\frac{\theta(t)}{2}\right] \mathbf{I} - i \sin\left[\frac{\theta(t)}{2}\right] \hat{r}(\Delta t) \cdot \boldsymbol{\sigma}, \quad (\text{B13})$$

where $\hat{r}(\Delta t) \stackrel{\text{def}}{=} \mathbf{r}(\Delta t) / \|\mathbf{r}(\Delta t)\|$ with $\mathbf{r} = \mathbf{r}(\Delta t)$ in Eq. (B12) and, in addition,

$$\cos\left[\frac{\theta(t)}{2}\right] = 1 - \frac{2}{N} \sin^2\left(\frac{\Delta t}{2}\right), \text{ and } \sin\left[\frac{\theta(t)}{2}\right] = \frac{2}{\sqrt{N}} \sin\left(\frac{\Delta t}{2}\right) \sqrt{1 - \frac{1}{N} \sin^2\left(\frac{\Delta t}{2}\right)}, \quad (\text{B14})$$

with $x = |\langle s|w \rangle| = 1/\sqrt{N}$ and N being the dimensionality of the search space. It is interesting to point out that since $\mathbf{r}\cdot\mathbf{s} = \mathbf{r}\cdot\mathbf{w} = x^2\cos(\Delta t/2)$, both $|s\rangle\langle s|$ and $|w\rangle\langle w|$ lie on the same circle of revolution about the \mathbf{r} -axis on the Bloch sphere. In summary, the action of each application of $U(\Delta t)$ is to rotate $|s\rangle\langle s|$ by an angle θ about the \mathbf{r} -axis. The procedure ends when enough rotations have been performed so that $|s\rangle\langle s|$ is near the solution $|w\rangle\langle w|$. Of course, there are multiple distinct ways of arriving at $|w\rangle\langle w|$ from $|s\rangle\langle s|$, depending on the choice of the simulation step length Δt that specifies the rotation angle $\theta(\Delta t)$ and the rotation axis $\hat{r}(\Delta t)$ given by

$$\hat{r}(\Delta t) = \frac{\cos\left(\frac{\Delta t}{2}\right)\left(\frac{\mathbf{s}+\mathbf{w}}{2}\right) + \sin\left(\frac{\Delta t}{2}\right)\left(\frac{\mathbf{s}\times\mathbf{w}}{2}\right)}{\left\| \cos\left(\frac{\Delta t}{2}\right)\left(\frac{\mathbf{s}+\mathbf{w}}{2}\right) + \sin\left(\frac{\Delta t}{2}\right)\left(\frac{\mathbf{s}\times\mathbf{w}}{2}\right) \right\|}. \quad (\text{B15})$$

From Eq. (B15) we note that $\hat{r}(\Delta t)$ belongs to the space spanned by $\{\mathbf{s}+\mathbf{w}, \mathbf{s}\times\mathbf{w}\}$. However, as reported in Refs. [27, 37], the optimal rotation would be the one in which $\hat{r}(\Delta t)$ belongs to the space spanned by $\{\mathbf{s}\times\mathbf{w}\}$. This, in turn, would imply choosing a $\Delta t = \pi$ in Eq. (B15). With this choice, the quantum simulation specified by $U(\Delta t)$ in Eq. (B1) equals $U(\pi) = e^{-i\pi|s\rangle\langle s|}e^{-i\pi|w\rangle\langle w|}$ with $e^{-i\pi|s\rangle\langle s|} = -\mathbf{s}\cdot\boldsymbol{\sigma} = \mathbf{I} - 2|s\rangle\langle s|$ and $e^{-i\pi|w\rangle\langle w|} = -\mathbf{w}\cdot\boldsymbol{\sigma} = \mathbf{I} - 2|w\rangle\langle w|$. Therefore, modulo a global phase shift, $U(\pi)$ is identical to Grover's iterate in a digital quantum search setting. With this final remark, we end our discussion here.

Appendix C: Derivation of Eq. (14)

In this appendix, we present fundamental elements of the Fubini-Study metric to facilitate the understanding of how to compute path lengths (i.e., Eq. (14)) in projective Hilbert space.

Let $\mathcal{H} = \mathcal{H}_2^n$ be an $N \stackrel{\text{def}}{=} 2^n$ -dimensional complex Hilbert space of n -qubit unit quantum states $\{|\psi\rangle\}$. Given the fact that the global phase of a vector state cannot be observed, a physical state can be represented by a so-called ray of the Hilbert space. The set of rays of \mathcal{H}_2^n defines the so-called complex projective Hilbert space $\mathcal{P}(\mathcal{H}) = \mathbb{C}P^{N-1}$. More formally, $\mathbb{C}P^{N-1}$ denotes the quotient set of \mathcal{H}_2^n by the equivalence relation $|\psi\rangle \sim e^{i\phi}|\psi\rangle$ with $\phi \in \mathbb{R}$. The space $\mathbb{C}P^{N-1}$ can be endowed with a mathematically valid and physically significant metric structure. In fact, let us consider a family $\{|\psi(\xi)\rangle\}$ of normalized quantum states of \mathcal{H}_2^n that vary smoothly with respect to an m -dimensional parameter $\xi \stackrel{\text{def}}{=} (\xi^1, \dots, \xi^m) \in \mathbb{R}^m$. Consequently, the standard Hermitian scalar product on \mathcal{H}_2^n gives rise to a metric tensor $g_{ab}(\xi)$ with $1 \leq a, b \leq m$ on the manifold of quantum states as defined as [49],

$$g_{ab}(\xi) \stackrel{\text{def}}{=} 4 \text{Re}[\langle \partial_a \psi(\xi) | \partial_b \psi(\xi) \rangle - \langle \partial_a \psi(\xi) | \psi(\xi) \rangle \langle \psi(\xi) | \partial_b \psi(\xi) \rangle], \quad (\text{C1})$$

where $\partial_a \stackrel{\text{def}}{=} \partial/\partial\xi^a$. The quantity $g_{ab}(\xi)$ in Eq. (C1) represents the so-called Fubini-Study metric tensor. Notably, we observe that this metric is positive definite, which is clear when examining the distance element ds_{FS}^2 between two adjacent points corresponding to the vector states $|\psi(\xi + d\xi)\rangle$ and $|\psi(\xi)\rangle$ [50],

$$ds_{\text{FS}}^2 \stackrel{\text{def}}{=} g_{ab}(\xi) d\xi^a d\xi^b = 4 \left[\langle d\psi | d\psi \rangle - |\langle \psi | d\psi \rangle|^2 \right], \quad (\text{C2})$$

with $|d\psi\rangle \stackrel{\text{def}}{=} |\psi(\xi + d\xi)\rangle - |\psi(\xi)\rangle$. The distance element ds_{FS}^2 in Eq. (C2) naturally introduces the idea of geodesic paths in $\mathbb{C}P^{N-1}$. For more details on the notion of Fubini-Study metric, we suggest Ref. [49].

To calculate path lengths, one needs to use $g_{ab}(\xi)$ in Eq. (C1). In particular, it can be shown that the quantum line between states $|A\rangle$ and $|B\rangle$ can be parametrized in terms of a single parameter $\xi \in [0, \pi]$ as [6],

$$|\psi(\xi)\rangle = \frac{\cos\left(\frac{\xi}{2}\right) |A\rangle + \frac{\langle B|A\rangle}{|\langle B|A\rangle|} \sin\left(\frac{\xi}{2}\right) |B\rangle}{\sqrt{1 + \sin(\xi) |\langle B|A\rangle|}}, \quad (\text{C3})$$

with $|\psi(0)\rangle = |A\rangle$ and $|\psi(\pi)\rangle \simeq |B\rangle$ (with “ \simeq ” denoting physical equivalence between quantum states, modulo irrelevant global phase factors). The parameter ξ is related to the temporal parameter t (adjusted in such a manner that $0 \leq t \leq 1$) by means of the relation $t(\xi) \stackrel{\text{def}}{=} \tan(\xi/2) / [1 + \tan(\xi/2)]$ so that $t(0) = 0$ and $t(\pi) = 1$. Then, the length $\mathcal{L}[\gamma(\xi)]_{0 \leq \xi \leq \pi} = \mathcal{L}[\gamma(\xi(t))]_{0 \leq t \leq 1}$ of the path $\gamma(\xi) : \xi \mapsto |\psi(\xi)\rangle$ with $0 \leq \xi \leq \pi$ equals

$$\mathcal{L}[\gamma(\xi)]_{0 \leq \xi \leq \pi} = \int_0^\pi \sqrt{g_{\text{FS}}(\xi)} d\xi = 2 \arccos[|\langle A|B\rangle|], \quad (\text{C4})$$

where $g_{\text{FS}}(\xi)$ in Eq. (C4) can be evaluated by inserting Eq. (C3) into Eq. (C1). This concludes our discussion regarding how to reach Eq. (14). For further technical specifications, we recommend referring to Ref. [6].